Autocrine S100B in Astrocytes Promotes VEGF-dependent Inflammation and Oxidative Stress, and Causes Impairment of Neuroprotection

xuebao wang
Wenzhou Medical University
he yu
Wenzhou Medical University
leping liu
Wenzhou Medical University
baihui chen
Wenzhou Medical University
shuya feng
Wenzhou Medical University
saidan ding (firstdsdan@hotmail.com)
The First Affiliated Hospital of Wenzhou Medical University https://orcid.org/0000-0003-1658-2319

Research article

Keywords: S100 calcium-binding protein B (S100B), Vascular endothelial growth factor (VEGF), inflammation, cognitive impairment, astrocytes

Posted Date: March 10th, 2021

DOI: https://doi.org/10.21203/rs.3.rs-263366/v1

Abstract

Background: Our previous study revealed that minimal hepatic encephalopathy (MHE) is strongly associated with neuroinflammation. Nevertheless, the underlying mechanism of the induction of inflammatory response in MHE astrocytes remains unclear.

Methods: In this study, we further investigated the effect and mechanism of S100B, predominant isoform expressed and released from mature astrocytes, on MHE-like neuropathology in the MHE rat model.

Results: We discovered that S100B expressions and autocrine were significantly increased in MHE rats and astrocytes isolated from MHE rats. Furthermore, we found that S100B stimulates VEGF expression via the interaction between TLR2 and RAGE in an autocrine manner. S100B-facilitated VEGF autocrine expression further led to a VEGFR2 and COX-2 interaction, which in turn induced the activation of NF□B, eventually resulting in inflammation and oxidative stress caused by MHE astrocytes. Compared to WT astrocytes, impairment of MHE astrocytes supported neuronal growth in co-culture.

Conclusions: To sum up, comprehensive-understanding of the impact of S100B-overexpressed MHE astrocyte on MHE pathology may provide insights into the etiology of MHE.

Background

Minimal hepatic encephalopathy (MHE) is characterized by a specific, complex mild cognitive impairment. Attention deficits, psychomotor slowing, and impaired bimanual and visuomotor coordination are among the few key features [1, 2]. A previous study has suggested that pro-inflammatory cytokines released from astrocytes participate in the regulation of pathogenesis of MHE [3]. However, the underlying mechanism of the induction of inflammatory response in MHE astrocytes remains unclear.

S100 calcium-binding protein B (S100B) is a predominant isoform of the S-100 protein family [4], mainly expressed and released from mature astrocytes [5][6]. Secreted S100B exerts an autocrine effect on astrocytes [7], being toxic at high concentrations [8]. Astrocytic S100B acts as a perpetrator of the noxious cytokine cycle, associated with maladaptive astrocytic activation [12][13]. Micromolar S100B levels, which can turn astrocytes into a pro-inflammatory neurodegenerative phenotype, are an important source of inflammatory cytokines [10] that induce TNFα secretion [9]. Overexpression and knockout of S100B have been associated with exacerbation and attenuation of brain damage, respectively [14]. The activated astrocytes' responses to neuronal damage or dysfunction reflected in AD brain markedly overexpress intercellular biologically active S100B [15][16]. However, so far, no studies have reported on the production of S100B by astrocytes in MHE rats and the underlying mechanism by the autocrine action of S100B on pro-inflammatory response.

Vascular endothelial growth factor A (VEGF-A) is the key member of the VEGF family [21], which interacts with VEGF receptor-1 (VEGFR1) and VEGFR2. As a permeability factor, excessive VEGF-A activates the inflammatory pathway [22], and its levels are elevated in many inflammatory diseases [17]. *In vitro* and *in*

vivo studies suggested that in inflammatory CNS disorders, VEGF-A and its receptors can be re-expressed by reactive astrocytes [18–20]. Current evidence suggests that functional VEGF receptors give rise to autocrine VEGF signaling [23]. Thus, although VEGF functions as a pro-inflammatory cytokine, it is responsible for the induction of inflammation [26, 27]. Much less is known about the effects of autocrine VEGF signaling on the induction of pro-inflammatory cytokine in astrocytes. In addition, previous studies have suggested that S100B at the micromolar level induces VEGF upregulation and secretion in cardiomyocytes [28]. We speculated that autocrine S100B might correlate well with autocrine VEGF and influenced inflammation depending on autocrine VEGF effects by MHE astrocytes.

The aim of this study was to investigate whether the S100B-dependent astrocytes impairment influences MHE-like neuropathology in the MHE rat model and whether overexpression of autocrine S100B, representative of functional impairments of astrocytes, causes stimulation (overproduction) of VEGF through an interaction of TLR2 with RAGE. In addition, we investigated whether autocrine S100B transducing activity might precede COX-2 activity, NF□B nuclear translocation, and inflammatory molecules expression depending on autocrine VEGF through parallel stimulation of VEGFR2/COX-2 interaction in astrocytes,

Materials And Methods

MHE models and treatment

Sprague-Dawley rats (220-250g, n=40) were obtained from the Experimental Animal Center of the Chinese Academy of Sciences in Shanghai. All the animals were housed in an environment with a temperature of 22 ± 1 ºC, relative humidity of 50 ± 1%, and a light/dark cycle of 12/12 hr. All animal studies (including the mice euthanasia procedure) were done in compliance with the regulations and guidelines of Wenzhou Medical University institutional animal care and conducted according to the AAALAC and the IACUC guidelines [29].

Prior to the experiment, all rats were subjected to the Y-maze (YM) task [30] and the water-finding task (WFT) [31] to obtain normal values of these behavioral tests. Intraperitoneal injection (IP) of TAA (200 mg/kg in normal saline; Sigma-Aldrich, St. Louis, MO, USA) was performed twice per week for 8 weeks. TAA-treated rats, which exhibited decreased motor activity, lethargy, and eventual progression to coma, were diagnosed as HE rats. TAA-treated rats with no HE symptoms, subjected to YM and WFT tests, were confirmed as MHE rats when YM value was lower or WFT value was higher than mean ± 1.96·SD.

Adult primary astrocytes culture

Cerebral cortexes of MHE or wild type rats were dissociated to single-cell suspensions in a papain based dissociation buffer (2.5 mM $CaCl_2$, 0.83 mM EDTA, 137 U papain (Sigma), 100 µl DNAse (Sigma), 3–5 crystals of Cysin HBSS-Hepes (20mM)). Percoll gradient (Sigma) was used to remove myelin and lyse red

blood cells. The remaining cells were plated in poly-D-lysine-coated 75 cm^2 culture flasks at a concentration of 15 $\times 10^6$ cells in 1% serum-containing DMEM/F12 medium for 72h. The medium was changed every 72h.

Adult primary astrocytes treatment

Adult primary astrocytes were exposed to S100B (final concentration of 0.1 and 2 μM, 1% DMSO), RAGE inhibitor FPS-ZM1 (250 nM), TLR2 inhibitor C29 (1μM), VEGFR inhibitor PTK787 (10 mM), COX-2 inhibitor celecoxib (40 μM), anti-VEGF antibody (AVAB, 1 mg/ml) or NF□B inhibitor PDTC (0.1 μmol/L) or anti-S100B antibody (ASAB, 250ng/ml). Otherwise, MHE astrocytes were transfected with S100B/VEGF siRNA or the Control siRNA plasmid (Santa Cruz, CA, USA) using Lipofectamine 2000 (Invitrogen, Carlsbad, CA, USA) for 24h according to the protocol suggested by the manufacturer.

Primary cortical neurons culture

Primary cortical neuron cultures were prepared from the freshly dissected cerebral cortex from 1-day-old rat pups and dissociated to single-cell suspensions using papain digestion. Then, cells were placed in poly-L-lysine-precoated six-well plates, and co-cultured with adult primary astrocytes cultured in the insert Transwell dishes (Millipore) in Neurobasal® Medium (1X) supplemented with 0.5 mM GlutaMAX™-I, B-27®for 24 h. The pore size of the membrane was 0.4 mm.

Neuroblastoma 2a (N2A) cells culture

N2A cells were placed in poly-L-lysine-precoated six-well plates and were cocultured with MHE astrocytes in the insert Transwell dishes (Millipore) in DMEM supplemented with 1mM sodium pyruvate, 4mM L-glutamine, 10% FCS, 100 U/ml penicillin, 0.1 mg/ml streptomycin (Biological Industries, Beit-Haemek, Israel).

NF□B -sensitive luciferase Assay

Astrocytes stably transfected with NF□B reporter gene and VEGF siRNA were cultured on 12-well plates. The cells were starved from serum overnight and then stimulated with S100B (2 μM) for 6h. The cells were lysed with 1×luciferase cell culture lysis reagent (Promega, Madison, WI). Supernatants from cell lysates were subjected to luciferase assay according to the manufacturer's instruction (Stratagene, LaJolla, CA). Briefly, 20 μl of supernatant were mixed with 100 μl of luciferase assay buffer (40mM Tricine, pH7.8, 0.5mM ATP, 10mM $MgSO_4$, 0.5mM EDTA,10mM 1,4-dithiothreitol, 0.5mM coenzyme A, and 0.5mM luciferin), and the intensity of luminescence was immediately measured using a luminometer (Lumat LB9507; Berthold Technologies, OakRidge, TN). Samples were assayed in triplicate, and the

luciferase activity was normalized based on protein concentrations of the cell lysate. The results are presented as ratios of relative light units of treatment groups to control groups.

Detection of COX-2 Activity

COX-2 Activity Assay Kit (Abcam Inc., Boston, MA, USA) was used to detect COX-2 activity in the homogenate of MHE astrocytes with S100B treatment in preincubation of PTK787 following the manufacturer’s instructions.

Real-time quantitative PCR (qPCR)

Total RNA was extracted using TRIzol reagent (Invitrogen). Briefly, 1 μg of total RNA was reverse transcribed into cDNA using Superscript II reverse transcriptase (Invitrogen). Real-time PCR was performed with SYBR Green mix (1:20,000 SYBR Green) on an iCycler iQ real-time detection system (BioRad) according to the manufacturer's instructions. Each reaction was performed in duplicate or triplicate on at least three samples for each condition, in a volume of 25 μl. The mRNA expression was quantified using the relative 2 (−ΔΔC(T)) method. Relative levels of mRNA were normalized to the values of GAPDH mRNA for each reaction. Each DNA sample was then separated by agarose gel. DNA fragments were subsequently visualized and photographed on a long wave UV lightbox. PCR primers are listed in Table 1.

Table 1
Sequences of used primers

Gene name	Sequence	
S100B	5'AGCTGGAGAAGGCCATGGTG3'	Forward
	5'GAACTCGTGGCAGGCAGTAG3'	Reverse
MAP2	5'CTGGACATCAGCCTCACTCA3'	Forward
	5'GCCTTCCTCCTCCTCTCTGT3'	Reverse
GFAP	5'GAGTTACCAGGAGGCACTCG3'	Forward
	5'ATGGTGATGCGGTTTTCTTC3'	Reverse
IBA1	5'CCATGAAGCCTGAGGAAATTTCA3'	Forward
	5'TTATATCCACCTCCAATTAGGGCA3'	Reverse
CD31	5'AGTGAGGTTCTGAGGGTGAAGG3'	Forward
	5'TCACTCCGATGATAACCACTGC3'	Reverse
O4	5'ACTATGGTTTGGCTATACTCCT3'	Forward
	5'ATTCATATCCTGCGTGGC3'	Reverse
VEGFa	5'-AACTTCTACCCGTGCCTT-3'	Forward
	5'- ACTTAGGTCAGCGTTTCC-3'	Reverse
RAGE	5'-GTCCAACTACCGAGTCTACC-3'	Forward
	5'-CCACCTTCAGGCTCAACCAACAG-3'	Reverse
COX-2	5'TTCAAATGAGATTGTGGGAAAAT3'	Forward
	5'AGATCATCTCTGCCTGAGTATCTT3'	Reverse
TLR2	5'-GGCTCACAGGCAAAATCACG-3'	Forward
	5'-CGAAGGTGTTGGAGCGAAAA-3'	Reverse
TLR4	5'-CTTTGAAAATGTAAGGCGGC-3'	Forward
	5'-ATGTAGGCAGGTGTGTGGG-3'	Reverse
VEGFR1	5'-CGCTTTTTGTCAGTCATCTTCA-3'	Forward
	5'-TCTCGGCATTCACTTTGGTC-3'	Reverse
VEGFR2	5'-TACACAATTCAGAGCGATGTGTGGT-3'	Forward
	5'-CTGGTTCCTCCAATGGGATATCTTC-3'	Reverse
GAPDH	5'-ACCCAGAAGACTGTGGATGG-3'	Forward

5'-ACACATTGGGGGTAGGAACA-3'	Reverse

Flow cytometry for evaluating cell apoptosis

N2A cells were co-cultured with adult primary astrocytes culture in an insert Transwell dish for 48 h and harvested. Harvested N2A cells were washed in PBS, then with Binding Buffer (1 mM HEPES, 14 mM NaCl, 2.5 mM $CaCl_2$ in PBS). Cells were then incubated in Binding Buffer containing PE-conjugated Annexin V (eBioscience, San Diego, CA) for 10 min at room temperature. Dead cells were detected with DAPI solution (0.1 μg/ml). BD FACSCanto™ II flow cytometer equipped with FacsDiva program was used for analysis.

ELISA assay

Enzyme-linked immunosorbent assay (ELISA) kits (R&D Systems, Minneapolis, MN, USA) were used to measure extracellular S100B/VEGF/TNFα levels in the culture medium of MHE astrocytes according to the manufacturer's recommendations. Levels of these cytokines were then analyzed using a Thermo Fisher Multiskan MCC plate reader (Waltham, MA, USA) by the spectrophotometrical method.

Immunoblotting (IB) analysis

The total proteins were separated by 10% SDS-PAGE and transferred to the PVDF membranes by electroblotting. The membranes were blocked by incubation in 5% non-fat dry milk dissolved in TBS-T (150 mM NaCl, 50 mM Tris, 0.05% Tween 20) for 1h, and incubated with primary antibodies: S100B, VEGFa, TLR2, TLR4, RAGE, NF□B, VEGFR1, VEGFR2, COX-2, TNFα, IL-1β, NOX1, NOX2 and β-actin (Abcam, Cambridge, UK) overnight at 4 °C. Samples were then incubated with horseradish peroxidase-conjugated secondary antibodies for 1h. Protein bands were visualized on Kodak BioMax films by ECL reagent (Thermo Fisher), scanned and subsequently densitometrically calculated using QuantityOne software. Densitometrical quantifications were indicated as fold change relative to control as fold of proteins to β-actin levels.

Co-immunoprecipitation

Cells lysates were incubated with TLR2, RAGE, VEGFR2, COX-2 antibodies overnight (4°C) and subsequently incubated with protein G-agarose beads (Millipore, Billerica, MA, USA) for 5 h (4°C). Beads were washed with lysis buffer. Immunoprecipitated proteins were resolved by SDS-PAGE and electroblotted. Proteins were probed using primary antibodies (TLR2, TLR4, RAGE, VEGFR1, VEGFR2, COX-2) and secondary antibodies.

Fluorescent staining

Four-micron frozen cerebral cortex sections on slides or cells cultured on glass coverslips were fixed with 4% paraformaldehyde for 30 min and blocked with PBS containing 3% BSA and 0.2% Triton-x 100 for 1 h. Samples were then incubated overnight at 4°C using the following primary antibodies: S100B, VEGFa, TLR2, TLR4, RAGE, NF□B, VEGFR1, VEGFR2, COX-2, TNFα, IL-1β, β-tubulin, MAP2, O4, IBA1, CD31, and GFAP (Abcam), and then with Alexa Fluor-488 (green)/594 (red)/350 (blue) conjugated secondary antibodies for 1h. For double-label staining of terminal deoxynucleotidyl transferase dUTP nick end labeling (TUNEL) with MAP2, primary cortical neuronal cultures on the coverslip were performed with TUNEL staining according to the manufacturer protocol (Roche, Switzerland) and incubated with antibody against MAP2 (Abcam) at 4°C overnight. Finally, samples were incubated with Alexa Fluor-594 (red) conjugated secondary antibodies for 1h. Images were viewed with a Leica TCS SP2 confocal laser scanning microscope.

Assessment of NADPH oxidase activity

Photon emission from the chromogenic substrate lucigenin as a function of acceptance of electron/O2- generated by the NADPH oxidase complex was measured at specific intervals in a Bioteck luminometer (Bioteck, USA). NADPH oxidase assay buffer containing 250 mM HEPES (pH7.4), 120 mM NaCl, 5.9 mM KCl, 1.2 mM $MgSO_4$ ($7H_2O$), 1.75 mM $CaCl_2$ ($2H_2O$), 11 mM glucose, 0.5mMEDTA, 100 µM NADH and 5µM lucigenin was used. The data were converted to relative light units/min/mg of protein. The lucigenin activity of MHE astrocytes homogenate from the control group was arbitrarily set at 100%.

ROS Detection Assay

MHE astrocytes were tested for reactive oxygen species generation using a ROS-ID Total ROS Detection Kit (Enzo Life Sciences) following manufacturer's protocol. Cells were treated with ROS detection reagent and incubated for 4h at 37°C in the dark. Following incubation, ROS level was analyzed via fluorescence microscopy. Obtained data were expressed as a percentage.

MTT assay

N2A cell viability was evaluated by MTT assay. Briefly, cells in 96-well plates were treated using a medium containing 0.5 mg/ml MTT at 37 °C for 3 h and then incubated using dimethylsulfoxide. The light absorption at 490 nm was measured by quantitative colorimetric assay with a microplate reader (TECAN).

Statistical analysis

All of the data were expressed as mean±SD. Data comparisons were analyzed using either Student's t-test (two-group comparison) or one-way analysis of variance (ANOVA) followed by Dunnett's post hoc multiple comparison test (more than two groups). $P < 0.05$ or $P < 0.01$ was considered as statistical significance.

Results

Astrocytes from MHE rats overexpress S100B

In astrocytes, S100B, a cytokine marker of astroglial activation in brain disorders, induces pro-inflammatory mediators' secretion [9]. Thus, we sought to determine whether S100B was elevated in astrocytes in neurological diseases MHE. We examined the expression of S100B using IB analysis and found that the expression of S100B was significantly increased in cortexes of MHE rats (Figure 1A and 1B). A maximal increase in S100B mRNA transcription was observed in cortexes (qPCR, Figure 1C and 1D), suggesting overexpression of S100B in the MHE brain.

To further investigate astrocytes' role in cortexes of MHE rats, we established adult astrocytes culture from MHE rats and WT rats. The astrocyte cell culture purity was analyzed by immunofluorescence staining with an astrocyte-specific marker (GFAP) and other cell-type-specific markers for neurons (MAP2), microglia (IBA1), endothelial cells (CD31), and oligodendrocytes (O4). We found that 99% of the cells were stained with GFAP (Figure 1E). We further evaluated our cell culture using RT-PCR by targeting these specific cell markers. We found that cultured astrocytes had an enriched expression of astrocyte-specific gene GFAP and low expression of other cell-type-specific genes compared to the whole brain (Figure 1F). Altogether, these experiments showed that this culture protocol generates a highly enriched astrocyte culture. Then, S100B production and secretion were assessed using IB analysis, qPCR, and ELISA assay. IB analysis and qPCR assay showed that MHE astrocytes showed a significantly higher S100B protein (Figure 1G and 1H) and mRNA expression (Figure 1I and 1J) compared to WT astrocytes. Moreover, an ELISA assay suggested that the level of S100B released from MHE astrocytes into the cell culture medium was obviously elevated compared to WT astrocytes (Figure 1K). Thus, we deduced there was an overload of S100B in MHE astrocytes.

Furthermore, to demonstrate the specificity of S100B in inflammation and oxidative stress, we inhibited S100B using an anti-S100B antibody in media and siRNA-induced-silencing in MHE astrocytes. We first tested the efficiency of S100B siRNA transfection into MHE astrocytes. As determined by qPCR, MHE astrocytes showed weak S100B expression after S100B siRNA transfection (Figure 1L) compared to control siRNA transfection, indicating efficient transfection. Then, we measured the inflammatory factors expression and secretion in MHE astrocytes. We found that the level of TNFα in the cell culture medium of MHE astrocytes was significantly increased compared to WT astrocytes. After knocking down the S100B in MHE astrocytes, the TNFα secretion was reduced or even inhibited (Figure 1M), indicating the induction of inflammation in MHE astrocytes by S100B.

MHE astrocytes are associated with S100B and VEGF production

Astrocyte-derived VEGF, as a pro-inflammatory cytokine [32], has a significant role in lesion pathogenesis of CNS disease characterized by inflammation [17, 33]. In this study, we investigated whether autocrine pro-inflammatory S100B from astrocytes affects the VEGF production and secretion. First of all, we examined the association of S100B and VEGF in MHE astrocytes *in vivo* and *in vitro*. Immunostaining of the MHE rat's brain revealed that S100B was colocalized with VEGFa in astrocytes (Figure 2A). Furthermore, confocal images from MHE astrocytes cultured *in vitro* showed colocalization of S100B with VEGF-A in the cytoplasm (Figure 2B).

Next, we addressed whether MHE astrocytes-derived S100B enhances VEGF production in an autocrine manner using S100B siRNA transfected-MHE astrocytes. IB and qPCR analysis showed significant elevation in VEGF protein (Figure 2C and 2D) and mRNA expressions (Figure 2E and 2F) in MHE astrocytes; however, these levels were decreased in cells transfected with S100B siRNA. Similar results were obtained from the ELISA assay; the cell culture medium of MHE astrocytes transfected with the control vector showed a significant increase in VEGF level, while S100B-deficient MHE astrocytes displayed decreased VEGF secretion (Figure 2G). Hence, our data suggested that autocrine S100B facilitated VEGF overproduction by MHE astrocytes.

Next, we assessed whether VEGF autocrine accumulation impacted the S100B expression in MHE astrocytes using VEGF siRNA transfection into MHE astrocytes. VEGF siRNA obviously decreased VEGF mRNA in MHE astrocytes by qPCR assay (Figure 2H), indicating successful transfection of VEGF siRNA. More importantly, IB analysis for S100B expression showed no change in S100B protein level after VEGF siRNA transfection in MHE astrocytes (Figure 2I and 2J). Additionally, the ELISA assay also showed that the level of S100B in the cell culture medium of MHE astrocytes was not altered after AVAB treatment (Figure 2K), indicating that changes in VEGF do not affect the S100B overload.

S100B-enhances VEGF production through a TLR2 and RAGE interaction

TLRs are involved in the release of inflammatory cytokines [34]. A previous study suggested that S100B protein binds to RAGE and, in turn, activates TLRs [35]. We estimated that autocrine S100B might trigger TLR activation via stimulation of RAGE, leading to VEGF production in MHE astrocytes. Thus, we tested the binding between RAGE and S100B *in vitro* using a coimmunoprecipitation experiment. The results showed that RAGE coimmunoprecipitated with S100B in MHE astrocytes (Figure 3A). We also validated this result by performing a reciprocal experiment using anti-rage, and found that RAGE and S100B physically interacted in MHE astrocytes (Figure 3A)

Next, we analyzed the association of RAGE with TLR in MHE rats *in vivo* using immunostaining experiments. Confocal images showed the co-localization of TLR2 with RAGE combined with GFAP in astrocytes in cortexes in MHE rats (Figure 3B), whereas the co-localization of TLR4 with RAGE was not found in astrocytes of cortexes (Figure 3C).

Furthermore, we tested the effect of S100B on the interaction between RAGE and TLR2 or TLR4 in MHE astrocytes *in vitro* using co-immunoprecipitation experiments. The results showed that RAGE was coimmunoprecipitated with TLR2 but no TLR4 in MHE astrocytes. We also validated this result by performing a reciprocal experiment using anti-TLR2. RAGE and TLR2 physically interacted, while RAGE failed to be coimmunoprecipitated with TLR2 after ASAB treatment (Figure 3D). Thus, we deduced that S100B elicits the RAGE and TLR2 but no RAGE and TLR4 interaction.

To assess whether S100B stimulates the VEGF expression through RAGE/TLR2 signaling, we incubated MHE astrocytes with RAGE inhibitor FPS-ZM1 and TLR2 inhibitor C29 preincubated with various concentration of S100B. Quantitative analysis by IB showed an increase in S100B-dependent VEGF production in a dose-response manner. To evaluate the contribution of RAGE and TLR2 interaction to S100B activity, we used RAGE inhibitor FPS-ZM1 and TLR2 inhibitor C29 in a competition assay. We discovered that FPS-ZM1 or C29 significantly reduced the effect of a high dose of S100B on VEGF expression in MHE astrocytes (Figure 3E and 3F). Similar results were found by ELISA assay; FPS-ZM1 or C29 dramatically decreased the high dose of S100B-induced VEGF secretion in MHE astrocytes (Figure 3G). Hence, we deduced that RAGE and TLR2 are required for S100B-mediated VEGF production.

Autocrine S100B-mediated VEGF triggers VEGFR2 and COX-2 interaction

The roles of VEGF receptors [39] and COX-2 [40] are associated with inflammatory processes. VEGFR2 participates in VEGF-mediated COX induction [41]. Therefore, we categorized the contribution of VEGFR2 or COX-2 to S100B-mediated VEGF activity. First, we used mouse anti-COX-2 and anti-GFAP antibodies combined with VEGFR1/2 to test the co-localization of VEGFR1/2 and COX-2 *in vivo*. Confocal images confirmed the presence of VEGFR2, but not VEGFR1, colocalized with COX-2 in the cortex astrocytes of MHE rats (Figure 4A and 4B). Next, we assessed the effect of S100B on the interaction between VEGFR and COX-2 in MHE astrocytes *in vitro* using co-immunoprecipitation analysis. As shown in Figure 4C, substantial COX-2 was coimmunoprecipitated with abundant VEGFR2 but not with VEGFR1. We also validated this result by performing a reciprocal experiment using anti-VEGFR2. Our result indicated that VEGFR2 and COX2 physically interacted in MHE astrocytes, whereas ASAB addition induced no interaction of VEGFR2 with COX2, thus suggesting that S100B facilitates the interaction of VEGFR2 with COX-2.

Next, to investigate whether VEGFR2/COX-2 signaling was implicated in S100B-mediated autocrine VEGF, we treated MHE astrocytes with AVAB or VEGF siRNA transfection in the presence of S100B. qPCR

analysis showed that AVAB decreased the VEGFR2 mRNA expression in MHE astrocytes (Figure 4D and 4E). Moreover, the knockdown of VEGF and AVAB attenuated the effect of S100B and decreased the expression of COX-2 (Figure 4F-H). Hence, our data indicated that VEGF is required for S100B-mediated VEGFR2/COX-2 signaling.

S100B-mediated activation of NF□B depends on autocrine VEGF by astrocyte

Nuclear factor kappa-light-chain-enhancer of activated B cells (NF□B), as a central transcription factor, has a major role in pro-inflammatory response[36]. Studies have found that S100B can induce nuclear translocation and transcriptional activity of NF□B (p65) [37][38]. However, the exact mechanism of S100B-mediated NF□B activation in an autocrine action still remained unclear. Thus, we examined the contribution of S100B autocrine to activation of NF□B in a competition assay. Immunoblots of cytoplasmic and nuclear NF□B protein showed that nuclear NF□B content was significantly increased in MHE astrocytes. Moreover, the addition of S100B substantially enhanced NF□B nuclear translocation. Then, we evaluated the contribution of VEGF to S100B activity. Silencing of VEGF by VEGF siRNA transfection significantly diminished S100B-mediated NF□B nuclear translocation in MHE astrocytes, indicating the involvement of VEGF in the S100B-response NF□B nuclear translocation (Figure 5A-C).

Next, we used a luciferase-based reporter gene construct to test an NF□B-sensitive gene transcription. NF□B-dependent transcription indeed was activated in MHE astrocytes, and the enhancement of transcriptional response was observed after treating cells with exogenous S100B. However, knockdown of VEGF effectively blocks the S100B-mediated activation of the NF□B-dependent transcription (Figure 5D), indicating the role of VEGF in the S100B-response NF□B activation.

To assess whether S100B affects NF□B activation through COX-2, we treated MHE astrocytes with S100B together with VEGFR2 inhibitor PTK787 or COX-2 inhibitor celecoxib. Immunostaining confirmed that NF□B was largely localized to the nucleus in S100B-treated MHE astrocytes. After AVAB, PTK787, or celecoxib treatment, NF□B was hardly detected in the cell nucleus (Figure 5E), suggesting an involvement of VEGFR2 and COX-2 in S100B-dependent NF□B nuclear translocation. We then examined the levels of pro-inflammatory factors using qPCR analysis. S100B induced an excessive TNFα level in MHE astrocytes, while AVAB addition significantly diminished S100B-induced TNFα production (Figure 5F and 5G), indicating the responsibility of VEGF for the S100B-induced inflammatory action.

S100B-mediated oxidative stress depends on autocrine VEGF by astrocytes

Elevated oxidative stress [22] and inflammation, [23] which have been associated with the severity of disease, have been reported in a variety of pathophysiological conditions. The linkage between increased

oxidative stress and acute-phase inflammation is already well understood [20]. Like inflammation, S100B is implicated in oxidative stress. In this study, we transfected MHE astrocytes with S100B siRNA to determine the contribution of S100B in oxidative stress. ROS production assay showed that ROS level was obviously increased in MHE astrocytes. However, the ROS production was significantly lowered with the knockdown of S100B (Figure 6A). Moreover, IB analysis of NADPH oxidase expression showed significant increases in NOX1/NOX2 level in MHE astrocytes, while the knockdown of S100B significantly reduced the protein expression (Figure 6B and 6C). In addition, analysis of NADPH oxidase activity displayed an obvious increase in MHE astrocytes, while ASAB treatment led to decreased activity (Figure 6D), indicating the induction of inflammation in MHE astrocytes by S100B.

The binding of VEGF to VEGFR2 results in a burst of ROS [60]. To examine whether S100B autocrine enhances the oxidative stress through VEGF autocrine in MHE astrocytes, we pre-incubated MHE astrocytes with S100B and then transfected cells with VEGF siRNA. The addition of S100B further amplified ROS production, while the silencing of VEGF lowered the levels of ROS in S100B-treated MHE astrocytes, indicating the responsibility of VEGF for the S100B-induced inflammatory action (Figure 7A). Moreover, the knockdown of VEGF significantly diminished the action of S100B, indicating the involvement of VEGF in the S100B-response NOX1 and NOX2 regulation (Figure 7B and 7C).

NF-kB up-regulates NADPH oxidase activity, leading to an increase in ROS levels [50]. COX2 contributes to oxidative stress [14] and regulates NADPHox-driven ROS production [44]. To assess the impact of S100B on the oxidative stress depending on COX-2 and NF□B, we treated MHE astrocytes with S100B together with NFKB inhibitor PDTC or COX-2 inhibitor celeCOXib. NADPH oxidase activity was significantly increased in MHE astrocytes; increased NADPH oxidase activity was further activated after treatment of exogenous S100B. However, PTK787, celeCOXib, PDTC, or AVAB addition diminished the effect of S100B (Figure 7D), indicating the involvement of COX-2/nfkb signaling in S100B-response oxidative stress.

MHE astrocytes have impaired ability to promote neuronal growth

Given the extensive dependency of neurons on astrocytic support (growth and viability)[42], we co-cultured N2A cells with MHE astrocytes to address the effect of the MHE astrocytes on the neuronal viability using MTT assay. MHE astrocytes resulted in obvious N2A cell loss after 18h and 24h of co-culturing (Figure 8A). Moreover, we evaluated the apoptotic effect of MHE astrocytes on N2A cells *in vitro* by flow cytometry. Flow cytometric analysis of apoptosis showed that the percentage of apoptotic neurons was significantly higher after co-culturing N2A cells with MHE astrocytes than with WT astrocytes (Figure 8B and 8C). Moreover, similar results were observed *in vivo.* Briefly, we isolated neurons from P1–P2 pups with co-cultured of MHE astrocytes to assess primary cortical neuronal apoptosis using the TUNEL study. Primary cortical neurons showed the obvious increase in TUNEL positive cells (apoptosis) in co-cultures with MHE astrocytes as compared to co-cultures with MHE astrocytes (Figure 8D).

We also characterized whether MHE astrocytes were impaired in promoting neurite growth length of the longest neurite per primary cortical neuron. Length of the longest neurite per neuron, evident by β-tubulin staining, was measured in at least 100 neurons per coverslip. We discovered that neurons had longer neurites in contact with WT astrocytes. MHE astrocytes promoted the growth of shorter neurites by co-cultures as compared to WT astrocytes culture (Figure 8E and 8F). These data indicated that activated astrocytes impair neuronal survival in MHE.

Discussion

This study determined an essential role of astrocyte dysfunction in MHE. Our data suggested a role of S100B in mediating astrocyte activity and MHE pathology via an autocrine manner. We found that S100B-induced pathological changes in astrocyte activity during MHE may accelerate inflammation. In addition, we discovered that the VEGF-dependent inflammation regulates the involvement of S100B in the pathogenesis of MHE. MHE astrocytes trigger neuronal impairment and halt the disease progression. We also found that MHE astrocytes maintained S100B overexpression *in vivo* and were functionally impaired in neuronal support, increasing VEGF expression. The autocrine mechanisms of S100B pro-inflammatory action were associated with the binding of the VEGF and VEGFR and the interaction of VEGFR and COX-2. In conclusion, we suggested that targeting S100B may result in disease-modifying therapies and might be used as a pharmacological approach for MHE.

The protein S100B is abundant in the nervous system and is mainly expressed in astrocytes [43]. S100B is secreted by astrocytes to the extracellular space [4], thereby affecting astrocytes in an autocrine manner and neurons in a paracrine manner [44]. Once released by astrocytes into the extracellular brain space, S100B exerts a dual effect on brain cells, acting as a neurotrophic factor at low (i.e., nanomolar) concentrations and as a toxic factor at high (i.e., micromolar) concentrations [43]. Micromolar S100B levels turn astrocytes into a pro-inflammatory neurodegenerative phenotype. Moreover, when activated, astrocytes can become an important source of inflammatory cytokines [10]. *In vitro* studies on astrocytes have suggested that excessive production of S100B has a pro-inflammatory effect leading to the secretion of tumor necrosis factor-alpha (TNFα) and subsequent enhanced inflammation [9]. Increases of brain S100B amount partly mimic pathological brain conditions in Down's syndrome, Alzheimer's disease, and other neuronal diseases [45, 46]. The constitutive overexpression of S100B might cause chronic neuronal damage [47]; thus, S100B has been considered a specific marker of brain tissue damage [48]. Moreover, transgenic mice overexpressing human S100B exhibits impaired hippocampal LTP and spatial learning [49]. However, studies have suggested that on the accumulation in the brain tissue and astrocytes from MHE rats, S100B may be a pathogenic factor to cause MHE pathology. Low S100B and RAGE were found in the brain of normal rats, and primary adult normal rats cultured astrocytes, while cortices and primary adult MHE rats cultured astrocytes showed excessive S100B and high TNFα expression. Knockdown of S100B in primary adult MHE rats' cultured astrocytes induced low TNFα levels, suggesting that the autocrine function of extracellular S100B affected astrocytes to stimulate the inflammatory cytokines production and secretion.

Vascular endothelial growth factors (VEGFs), as a pro-inflammatory cytokine, are implicated in generating clinical deficits of many chronic inflammatory diseases [17, 73, 32]. Notably, astrocytes stimulate basal levels of VEGF secretion under normal physiological conditions [74]. Reactive astrocytes result in VEGF-A overproduction in CNS inflammatory disease [33, 75]. Recent studies have found functional autocrine VEGF/VEGF receptor loops in many types of cells, such as hematopoietic stem cells (HSC) [76], human leukemia cells [77], osteosarcoma cells [78], and malignant cells [25, 79]. VEGF and its receptors (VEGF receptor-1, -2, and -3 (VEGFR1-3)), can be expressed in astrocytes [20]. The role of VEGF and its receptors are more related to inflammation [39]. The endogenous secreted S100B from astrocytes appears to be sufficient to induce VEGF secretion from astrocytes in an autocrine-dependent manner, while the elevation of VEGF does not affect S100B secretion. Autocrine extracellular S100B interacts with RAGE, thus affecting the VEGF production and secretion from astrocytes. We showed that S100B essentially elicited the inflammatory reaction due to VEGF mediation in an autocrine-dependent manner in MHE astrocytes.

The cell surface receptor for S100B on astrocytes mediating the autocrine effects has not been identified so far. Receptor for AGE (RAGE) has been reported to be a multiligand member of the immunoglobulin superfamily of receptors [54] that engages with various ligands, including members of the S100 family S100B, and is implicated in the expression of the receptor itself [55]. RAGE receptor has been involved in intracellular signal transduction [53]. RAGE recruitment in astrocytes [56, 57] has been identified as a responsible receptor mediating autocrine S100B effects [58]. RAGE recruitment by ligand has been found to be directly involved in facilitating the resolution of cellular pro-inflammatory responses [59], resulting from the activation of the pro-inflammatory transcription factor nucleus factor-kappa-light-chain enhancer of activated B cells (NFκB) [60], leading to the expression of TNFα [61]. Elevated RAGE expression was reported to be related to many inflammatory conditions or tissue injury [62, 63]. *In vivo* and *in vitro* results showed that RAGE expression in MHE astrocytes was decreased by knockdown of S100B. We also found that S100B was colocalized with RAGE in the cortex of MHE rats, while in astrocytic S100B has been shown to interact with RAGE to induce the pro-inflammatory mediators. It was observed that autocrine S100B discretely interacted with RAGE in the cytoplasm in MHE astrocytes. Thus, we believe that astrocytes expressing RAGE are a target of S100B. In MHE, astrocytes S100B's ability have been shown to activate astrocytes and induce the RAGE engagement through an autocrine mechanism. Thus, the S100B's ability to activate astrocytes via RAGE engagement and upregulate RAGE expression in astrocytes might significantly contribute to neuroinflammation.

Toll-like receptors (TLRs), a family of type 1 transmembrane proteins [64], have a critical role in the inflammatory response. Convergence and amplification of RAGE and TLR signaling sustain and amplify inflammatory responses [66][67]. Previous studies have found that S100B protein is also involved in the TLR signaling pathway by interaction with RAGE [34, 35]. S100B-exposed astrocytes showed a pro-inflammatory phenotype with the expression of pro-inflammatory TLR2 [68, 69]. Previous studies have shown that high levels of TLR4 and RAGE are associated with neuroinflammation [65]. Several studies have suggested that RAGE/TLR2 physical association is involved in S100B–induced cellular effects [70]. Emerging evidence suggests that S100B is sufficient to mediate TLR2 upregulation but not TLR4 expression in MHE astrocytes. Thus, RAGE/TLR2 might be a complex receptor mediating autocrine

S100B effects. We also found that S100B stimulates the overproduction of pro-inflammatory mediator VEGF via TLR2 and RAGE interaction in MHE astrocytes. Based on these findings, we suggest that S100B acts in an autocrine manner by mediating the expression and secretion of potent inducers of inflammation through a RAGE and TLR2 interaction. High S100B induced interaction between TLR2 and RAGE to promote the production of VEGF.

Cyclo-oxygenase 2 (COX-2) is an immediate-early response gene that exerts its key pro-inflammatory role by promoting an inflammatory process [80, 81]. Nonetheless, COX-2 expression in the brain has been associated with pro-inflammatory activities that are thought to be instrumental in the neurodegenerative processes of several acute and chronic diseases [40]. S100B can upregulate the pro-inflammatory enzyme COX-2 expression via RAGE engagement [80, 82-84]. Specifically, VEGF-dependent COX-2 induction is mediated through the VEGFR2 [41]. In this study, we demonstrated that S100B mediates VEGF-A molecules' expression and stimulates VEGFR1 and VEGFR2 overexpression in an autocrine fashion in MHE astrocytes. S100B-induced upregulation of COX-2 has shown to be dependent on VEGF engagement. VEGF binding results in VEGFR2 no VEGFR1 interaction with COX-2. S100B can trigger COX-2 activity via VEGFa-mediated VEGFR2. These protein interactions are essential for mediating intracellular inflammatory signaling.

NFκB is a tightly regulated transcription factor that induces several genes, including TNFα [85]. S100B can stimulate NF□B transcriptional activity [70], depending on RAGE [38]. The inhibition of NF□B results in significant suppression of S100B-induced TNFα expression [86]. RAGE is involved in cellular pro-inflammatory responses [55] resulting from the activation of the NFκB [87], including the expression of TNFα [88]. In the present study, we found that VEGF acts upstream of the nuclear translocation of NF□B (p65) and enhances NF□B (p65) transcriptional activity in the S100B-mediated inflammatory signaling pathway. Under stimulation by its ligands S100B and accumulation of VEGF, RAGE activates COX-2 signaling cascade, thereby evoking unrestrained NF□B nuclear translocation NF□B-transcriptional activity. COX-2 appears to act upstream of the nuclear translocation of NF□B (p65) and enhances NF□B (p65) transcriptional activity. Specifically, S100B-dependent modulation of VEGF expression binds VEGFR2 to enhance the nuclear translocation and transcriptional activity of NF□B (p65). S100B-induced RAGE via TLR2 ligation functions in an autocrine manner to elicit the downstream VEGF overproduction in the setting of interaction of VEGFR with COX-2, leading to the enhancement of COX-2 activity.

Existing studies have shown that cell-cell communication between primary neurons and astrocytes is crucial for the development, repair, and metabolism of neuronal systems [89]. Available evidence indicates that astrocytes exert the capability to synthesize and release soluble paracrine factors to surrounding neurons to promote neuron growth and survival [90]. One of the most important functions of astrocytes is the regulation of neurite growth. Astrocytes promote neurite growth by providing various diffusible and nondiffusible proteins [91]. Our data further demonstrated astrocytic impairment in neuronal support at the functional level; MHE astrocytes induced less neurite growth when co-cultured with neonatal neurons compared to WT astrocytes. Primary neurons co-cultured randomly with MHE astrocytes showed an increased sensitivity to the toxicity as compared to pure neuronal cultures. Thus,

MHE astrocytes could exert detrimental effects on neuronal growth. Higher TNFα expression by MHE astrocytes might account for the neuronal growth defects found in our co-culture experiments. As the inflammatory response from astrocytes might cause marked changes in neuronal survival and growth, detailed analysis of the composition of factors secreted from WT and MHE astrocytes is needed to gain a better understanding of mechanisms through which astrocytes affect neuronal survival in MHE.

Conclusion

Above all, accumulating evidence demonstrated that astrocytic S100B triggers the secretion of VEGF in an autocrine manner, which then regulates the secretion of inflammatory cytokines in an autocrine manner. VEGF has a vital role in the perpetuation of S100B-induced potent inflammatory response found in MHE astrocytes. Our results suggest that the S100B-enhancing effects of VEGF occur due to interaction between RAGE and TLR2 in MHE astrocytes. The present study indicated that the autocrine-dependent effect of VEGF might, in part, mediate the interaction of VEGFR2 with COX-2, thereby promoting the activation of NF□B and leading to inflammatory response and oxidative stress in animals' models of MHE disease (Fig. 8). In conclusion, S100B may be a potential pathological factor for MHE, achieving the inflammatory effect via VEGF mediation in astrocytes, which in turn irritates the impairment of neuronal survival.

Abbreviations

AAALAC: The Association for Assessment and Accreditation of Laboratory Animal Care International; AD: Alzheimer's disease; ANOVA: one-way analysis of variance; BSA: Albumin from bovine serum; CNS: central nervous system; COX-2: cyclo-oxygenase 2 ; DAPI: 4'6-diamidino-2-phenylindole; DMEM: Dulbecco's Modified Eagle Medium; DMSO: Dimethyl Sulphoxide; DNAse: deoxyribonuclease; EDTA: Ethylene Diamine Tetraacetic Acid; ELISA: Enzyme-linked immunosorbent assay; FCS: fetal calf serum; GAPDH: glyceraldehyde-3-phosphate dehydrogenase; GFAP: glial fibrillary acidic protein; HBSS: Hank's Balanced Salt Solution; HSC: hematopoietic stem cells; IACUC: Institutional Animal Care and Use Committee; IB: immunoblotting; IL-1β: Interleukin-1β; IP: intraperitoneal injection; LTP: longterm potentiation; MAP2: microtubule-associated protein 2; MHE: minimal hepatic encephalopathy; N2A: neuroblastoma 2a; NF□B: nuclear factor kappa-B; NOX: NADPH oxidase; PBS: phosphate buffer saline; PDTC: pyrrolidinedithiocarbamic acid; PVDF: Polyvinylidene Fluoride; qPCR: Real-time quantitative PCR; RAGE: advanced glycation end product receptor; S100B: S100 calcium-binding protein B; SDS-PAGE: sodium dodecyl sulfate polyacrylamide gelelectrophoresis; SiRNA: small interfering RNA; TAA: thioacetamide; TLR2: toll-like receptor 2; TNFα: Tumor Necrosis Factor α; TUNEL: transferase dUTP nick end labeling; VEGF: vascular endothelial growth factor; VEGF-A: vascular endothelial growth factor A; VEGFR1: vascular endothelial growth factor receptor 1; VEGFR2: vascular endothelial growth factor receptor 2; WFT:water-finding task; WT:wild-type; YM task:Y-maze task

Declarations

Ethics approval and consent to participate

The study was approved by the Ethics Committee of the First Affiliated Hospital of Wenzhou Medical University.

Consent for publication

Not applicable

Availability of supporting data

The data that support the findings of this study are available from the corresponding author upon reasonable request.

Competing interests

The authors have declared no conflict of interest.

Funding

This study was supported by Basic Scientific Research Projects of Wenzhou city (Y20180076)Natural Science Foundation of Zhejiang province (LY21H030012) and Natural Science Foundation of China (81671042, 81300308).

Authors‘ Contributions

Saidan Ding supervised the entire project, designed the research and analysed the data and critically revised the manuscript. Shuya Feng and Baihui Chen conceived and designed the experiments, performed the research interpreted, and analysed the data, and wrote the paper. Xuebao Wang conceived and designed the experiments, interpreted and analysed the data, and supervised all the experimental procedure. Leping Liu and He Yu performed the research and analysed the data. All authors read and approved the final manuscript.

Acknowledgments

We thank Dr. Haoqi Ni for optimizing the image analysis method. We thank Dr. Yangping Shentu for technical supports. We thank Dr. Yunchang Mo for critical reading of the manuscript.

References

1. Amodio P, Montagnese S, Gatta A, Morgan MY. Characteristics of minimal hepatic encephalopathy. Metabolic brain disease. 2004;19(3-4):253-67.
2. Montoliu C, Piedrafita B, Serra MA, del Olmo JA, Ferrandez A, Rodrigo JM, et al. Activation of soluble guanylate cyclase by nitric oxide in lymphocytes correlates with minimal hepatic encephalopathy in cirrhotic patients. JouRNAl of molecular medicine. 2007;85(3):237-45.
3. Ding S, Wang W, Wang X, Liang Y, Liu L, Ye Y, et al. Dopamine Burden Triggers Neurodegeneration via Production and Release of TNF-alpha from Astrocytes in Minimal Hepatic Encephalopathy. Molecular neurobiology. 2016;53(8):5324-43.
4. Van Eldik LJ, Zimmer DB. Secretion of S-100 from rat C6 glioma cells. Brain Research. 1987;436(2):367-70.
5. Wang DD, Bordey A. The astrocyte odyssey. Progress in Neurobiology. 2008;86(4):342-67.
6. Wilder PT, Varney KM, Weiss MB, Gitti RK, Weber DJ. Solution structure of zinc- and calcium-bound rat S100B as determined by nuclear magnetic resonance spectroscopy. Biochemistry. 2005;44(15):5690.
7. Heizmann CW. Ca 2+ -Binding S100 Proteins in the Central Nervous System. Neurochemical Research. 1999;24(9):1097-100.
8. Zimmer DB, Cornwall EH, Landar A, Song W. The S100 protein family: history, function, and expression. Brain Research Bulletin. 1995;37(4):417.
9. Hu J, Van Eldik LJ. S100 beta induces apoptotic cell death in cultured astrocytes via a nitric oxide-dependent pathway. Biochimica Et Biophysica Acta. 1996;1313(3):239.
10. Ronaldson PT, Davis TP. Blood-brain barrier integrity and glial support: mechanisms that can be targeted for novel therapeutic approaches in stroke. Current Pharmaceutical Design. 2012;18(25):-.
11. Qin H, Benveniste EN. ELISA Methodology to Quantify Astrocyte Production of Cytokines/Chemokines In Vitro. Methods Mol Biol. 2012;814(814):235-49.
12. T M, T M, N T, Y K, S S, N K, et al. Astrocytic activation and delayed infarct expansion after permanent focal ischemia in rats. Part I: Enhanced astrocytic synthesis of S-100β in the periinfarct area precedes delayed infarct expansion. J Cereb Blood Flow Metab. 2002;22(6):711-22.
13. Mrak RE, C WSTGB. The role of activated astrocytes and of the neurotrophic cytokine S100B in the pathogenesis of Alzheimer's disease. Neurobiology of Aging. 2001;22(6):915-22.
14. Wainwright MS, Craft JM, Griffin WST, Alexander M, Jose P, Padgett KR, et al. Increased susceptibility of S100B transgenic mice to perinatal hypoxia-ischemia. Annals of Neurology. 2010;56(1):61-7.
15. Mrak RE, Sheng JG, Griffin WS. Correlation of astrocytic S100 beta expression with dystrophic neurites in amyloid plaques of Alzheimer's disease. JouRNAl of Neuropathology & Experimental Neurology. 1996;55(3):273.
16. Marshak DR, Pesce SA. Increased S100β neurotrophic activity in Alzheimer's disease temporal lobe. Neurobiology of Aging. 1992;13(1):1-7.

17. Baker PN, Krasnow J, Roberts JM, Yeo KT. Elevated serum levels of vascular endothelial growth factor in patients with preeclampsia ***. Obstetrics & Gynecology. 1995;86(5):815-21.
18. Dobrogowska DH, Lossinsky AS, TaRNAwski M, Vorbrodt AW. Increased blood-brain barrier permeability and endothelial abnormalities induced by vascular endothelial growth factor. JouRNAl of Neurocytology. 1998;27(3):163-73.
19. Proescholdt MA, Jacobson S, Tresser N, Oldfield EH, Merrill MJ. Vascular endothelial growth factor is expressed in multiple sclerosis plaques and can induce inflammatory lesions in experimental allergic encephalomyelitis rats. JouRNAl of Neuropathology & Experimental Neurology. 2002;61(10):914-25.
20. Kaur C, ., Sivakumar V, ., Zhang Y, ., Ling EA. Hypoxia-induced astrocytic reaction and increased vascular permeability in the rat cerebellum. Glia. 2010;54(8):826-39.
21. Bagri A, Tessier-Lavigne M. Neuropilins as Semaphorin Receptors2002.
22. Shim JW, Madsen JR. VEGF Signaling in Neurological Disorders. InteRNAtional JouRNAl of Molecular Sciences. 2018;19(1):275.
23. Barr MP, Bouchier-Hayes DJ, Harmey JJ. Vascular endothelial growth factor is an autocrine survival factor for breast tumour cells under hypoxia. InteRNAtional jouRNAl of oncology. 2008;32(1):41-8.
24. Vincent L, Jin DK, Karajannis MA, Shido K, Hooper AT, Rashbaum WK, et al. Fetal stromal-dependent paracrine and intracrine vascular endothelial growth factor-a/vascular endothelial growth factor receptor-1 signaling promotes proliferation and motility of human primary myeloma cells. Cancer Res. 2005;65(8):3185-92. Epub 2005/04/19.
25. Lee TH, Seng S, Sekine M, Hinton C, Fu Y, Avraham HK, et al. Vascular endothelial growth factor mediates intracrine survival in human breast carcinoma cells through inteRNAlly expressed VEGFR1/FLT1. PLoS medicine. 2007;4(6):e186. Epub 2007/06/07.
26. Miyamoto K, Khosrof S, Bursell SE, Moromizato Y, Aiello LP, Ogura Y, et al. Vascular endothelial growth factor (VEGF)-induced retinal vascular permeability is mediated by intercellular adhesion molecule-1 (ICAM-1). American JouRNAl of Pathology. 2000;156(5):1733.
27. Gille H, Kowalski J, Li B, Lecouter J, Moffat B, Zioncheck TF, et al. Gille, H. et al. Analysis of biological effects and signaling properties of Flt-1 (VEGFR-1) and KDR (VEGFR-2). A reassessment using novel receptor-specific vascular endothelial growth factor mutants. J. Biol. Chem. 276, 3222-3230. JouRNAl of Biological Chemistry. 2001;276(5):3222-30.
28. Tsoporis JN, Marks A, Haddad A, Dawood F, Liu PP, Parker TG. S100B Expression Modulates Left Ventricular Remodeling After Myocardial Infarction in Mice. Circulation. 2005;111(5):598-606.
29. Albrecht J, Hilgier W, Zielinska M, Januszewski S, Hesselink M, Quack G. Extracellular concentrations of taurine, glutamate, and aspartate in the cerebral cortex of rats at the asymptomatic stage of thioacetamide-induced hepatic failure: modulation by ketamine anesthesia. Neurochemical research. 2000;25(11):1497-502.
30. Yamada M, Chiba T, Sasabe J, Nawa M, Tajima H, Niikura T, et al. Implanted cannula-mediated repetitive administration of Abeta25-35 into the mouse cerebral ventricle effectively impairs spatial working memory. Behav Brain Res. 2005;164(2):139-46.

31. Kawasumi M, Chiba T, Yamada M, Miyamae-Kaneko M, Matsuoka M, Nakahara J, et al. Targeted introduction of V642I mutation in amyloid precursor protein gene causes functional abnormality resembling early stage of Alzheimer's disease in aged mice. Eur J Neurosci. 2004;19(10):2826-38.
32. Byzova TV, Goldman CK, Pampori N, Thomas KA, Bett A, Shattil SJ, et al. A Mechanism for Modulation of Cellular Responses to VEGF : Activation of the Integrins. Molecular Cell. 2000;6(4):851-60.
33. Weis SM, Cheresh DA. Pathophysiological consequences of VEGF-induced vascular permeability. Nature. 2005;437(7058):497-504.
34. Giuseppe E, Carla C, Giovanni S, Daniele DF, Francesco Paolo DA, Alba R, et al. Enteric glial-derived S100B protein stimulates nitric oxide production in celiac disease. Gastroenterology. 2007;133(3):918-25.
35. Tian J, Avalos A, Mao S, Chen B, Senthil K, Wu H, et al. Toll-like receptor 9-dependent activation by DNA-containing immune complexes is mediated by HMGB1 and RAGE. Nature Immunology. 2007;8(5):487-96.
36. Uwe S. NF-kappaB in critical diseases: a bad guy? Intensive Care Medicine. 2003;29(11):1873.
37. Hofmann MA, Drury S, Fu C, Qu W, Taguchi A, Lu Y, et al. RAGE Mediates a Novel Proinflammatory Axis : A Central Cell Surface Receptor for S100/Calgranulin Polypeptides. Cell. 1999;97(7):889-901.
38. Arumugam T, Simeone DM, Schmidt AM, Logsdon CD. S100P Stimulates Cell Proliferation and Survival via Receptor for Activated Glycation End Products (RAGE). JouRNAl of Biological Chemistry. 2004;279(7):5059-65.
39. Saban R, Simpson C, Davis CA, Dozmorov I, Maier J, Fowler B, et al. Transcription factor network downstream of protease activated receptors (PARs) modulating mouse bladder inflammation. BMC Immunology,8,1(2007-08-17). 2007;8(1):17.
40. Harris SG, Padilla J, Koumas L, Ray D, Phipps RP. Prostaglandins as modulators of immunity. Trends in Immunology. 2002;23(3):144-50.
41. Smith CJ, Zhang Y, ., Koboldt CM, Muhammad J, ., Zweifel BS, Shaffer A, ., et al. Pharmacological analysis of cyclooxygenase-1 in inflammation. Proceedings of the National Academy of Sciences of the United States of America. 1998;95(22):13313-8.
42. Müller HW, Seifert W. A neurotrophic factor (NTF) released from primary glial cultures supports survival and fiber outgrowth of cultured hippocampal neurons. JouRNAl of Neuroscience Research. 1982;8(2-3):195.
43. Donato R. S100: a multigenic family of calcium-modulated proteins of the EF-hand type with intracellular and extracellular functional roles. InteRNAtional JouRNAl of Biochemistry & Cell Biology. 2001;33(7):637-68.
44. Scotto C, Mély Y, Ohshima H, Garin J, Cochet C, Chambaz E, et al. Cysteine oxidation in the mitogenic S100B protein leads to changes in phosphorylation by catalytic CKII-alpha subunit. JouRNAl of Biological Chemistry. 1998;273(7):3901-8.

45. Van Eldik LJ, Wainwright MS. The Janus face of glial-derived S100B: beneficial and detrimental functions in the brain. Restor Neurol Neurosci. 2003;21(3-4):97-108.
46. Griffin WS, Stanley LC, Ling C, White L, Macleod V, Perrot LJ, et al. Brain interleukin 1 and S-100 immunoreactivity are elevated in Down syndrome and Alzheimer disease. Proceedings of the National Academy of Sciences of the United States of America. 1989;86(19):7611-5.
47. Reeves RH, Yao J, Crowley MR, Buck S, Zhang X, Yarowsky P, et al. Astrocytosis and axonal proliferation in the hippocampus of S100B transgenic mice. Proceedings of the National Academy of Sciences of the United States of America. 1994;91(12):5359-63.
48. Araque A, Carmignoto G, Haydon PG. Dynamic signaling between astrocytes and neurons. Annual Review of Physiology. 2001;63(1):795-813.
49. Gerlai R, Wojtowicz JM, Marks A, Roder J. Overexpression of a calcium-binding protein, S100 beta, in astrocytes alters synaptic plasticity and impairs spatial learning in transgenic mice. Learning & Memory. 1995;2(1):26.
50. Bianchi R, Kastrisianaki E, Giambanco I, Donato R. S100B protein stimulates microglia migration via RAGE-dependent up-regulation of chemokine expression and release. JouRNAl of Biological Chemistry. 2011;286(286):7214-26.
51. Ponath G, Schettler C, Kaestner F, Voigt B, Wentker D, Arolt V, et al. Autocrine S100B effects on astrocytes are mediated via RAGE. JouRNAl of Neuroimmunology. 2007;184(1):214-22.
52. Glezer I, Simard AR, Rivest S. Neuroprotective role of the innate immune system by microglia. Neuroscience. 2007;147(4):867-83.
53. Huttunen HJ, Fages C, Rauvala H. Receptor for Advanced Glycation End Products (RAGE)-mediated Neurite Outgrowth and Activation of NF-κB Require the Cytoplasmic Domain of the Receptor but Different Downstream Signaling Pathways. JouRNAl of Biological Chemistry. 1999;274(28):19919-24.
54. Neeper M, ., Schmidt AM, Brett J, ., Yan SD, Wang F, ., Pan YC, et al. Cloning and expression of a cell surface receptor for advanced glycosylation end products of proteins. JouRNAl of Biological Chemistry. 1992;267(21):14998-5004.
55. Hofmann MA, Drury S, Fu C, Qu W, Taguchi A, Lu Y, et al. RAGE mediates a novel proinflammatory axis: a central cell surface receptor for S100/calgranulin polypeptides. Cell. 1999;97(7):889-901.
56. Adami C, Bianchi R, Pula G, Donato R. S100B-stimulated NO production by BV-2 microglia is independent of RAGE transducing activity but dependent on RAGE extracellular domain. Biochimica Et Biophysica Acta. 2004;1742(1):169-77.
57. Alejandro V, Rocío S, Agustina GT, Gerardo R, Maria Florencia A, Alicia R, et al. S100B protein activates a RAGE-dependent autocrine loop in astrocytes: implications for its role in the propagation of reactive gliosis. JouRNAl of Neurochemistry. 2014;131(2):190.
58. Ranuncolo SM, Ladeda V, Gorostidy S, Morandi A, Varela M, Lastiri J, et al. Expression of CD44s and CD44 splice variants in human melanoma. Oncology Reports. 2002;9(1):51-6.

59. Shin YJ, Choi JS, Choi JY, Hou Y, Cha JH, Chun MH, et al. Induction of vascular endothelial growth factor receptor-3 mRNA in glial cells following focal cerebral ischemia in rats. JouRNAl of Neuroimmunology. 2010;229(1):81-90.
60. Yan SD, Chen X, Fu J, Chen M, Zhu H, Roher A, et al. RAGE and amyloid-|[beta]| peptide neurotoxicity in Alzheimer's disease. Nature. 1996;382(6593):685-91.
61. G L, M M, T S, P T, C F, T K, et al. Advanced glycation end products activate endothelium through signal-transduction receptor RAGE: a mechanism for amplification of inflammatory responses.%A Basta G. Circulation. 2002;105(7):816-22.
62. Chavakis T, Bierhaus A, Nawroth PP. RAGE (receptor for advanced glycation end products): a central player in the inflammatory response. Microbes & Infection. 2004;6(13):1219-25.
63. Stewart, I. B, Potts, J. E, McKenzie, D. C, et al. CAN ALTERED BODY POSITION ALLEVIATE THE POST-EXERCISE PULMONARY DIFFUSING CAPACITY IMPAIRMENT? Medicine & Science in Sports & Exercise. 1998;30(Supplement).
64. Mousa KK, Louise J, Ogg GS, Damo X, Liew FY. TLR2 is expressed on activated T cells as a costimulatory receptor. Proceedings of the National Academy of Sciences of the United States of America. 2004;101(9):3029-34.
65. Koprnová J, Svetlanský I, Babel'A R, Bilíková E, Hanzen J, Zuscáková IJ, et al. Prospective study of antibacterial susceptibility, risk factors and outcome of 157 episodes of Acinetobacter baumannii bacteremia in 1999 in Slovakia. Scandinavian JouRNAl of Infectious Diseases. 2001;33(12):891.
66. Masakiyo S, Hitoshi M, Ken-Ichi Y, Tomoyuki O, Yoshihiko S, Akira M, et al. TIRAP, an adaptor protein for TLR2/4, transduces a signal from RAGE phosphorylated upon ligand binding. Plos One. 2011;6(8):e23132.
67. Beijnum JRV, Buurman WA, Griffioen AW. Convergence and amplification of toll-like receptor (TLR) and receptor for advanced glycation end products (RAGE) signaling pathways via high mobility group B1 (HMGB1). Angiogenesis. 2008;11(1):91-9.
68. Villarreal A, Seoane R, González TA, Rosciszewski G, Angelo MF, Rossi A, et al. S100B protein activates a RAGE-dependent autocrine loop in astrocytes: implications for its role in the propagation of reactive gliosis. JouRNAl of Neurochemistry. 2014;131(2):190.
69. Selinfreund RH, Barger SW, Welsh MJ, Van Eldik LJ. Antisense inhibition of glial S100 beta production results in alterations in cell morphology, cytoskeletal organization, and cell proliferation. JouRNAl of Cell Biology. 1990;111(5):2021-8.
70. Adami C, Bianchi R, Pula G, Donato R. S100B-stimulated NO production by BV-2 microglia is independent of RAGE transducing activity but dependent on RAGE extracellular domain. Biochimica Et Biophysica Acta Molecular Cell Research. 2004;1742(1):169-77.
71. Ma W, Lee SE, Guo J, Qu W, Hudson BI, Schmidt AM, et al. RAGE ligand upregulation of VEGF secretion in ARPE-19 cells. Invest Ophthalmol Vis Sci. 2007;48(3):1355-61.
72. Tsoporis JN, Izhar S, Leongpoi H, Desjardins JF, Huttunen HJ, Parker TG. S100B Interaction With the Receptor for Advanced Glycation End Products (RAGE). Circulation Research. 2010.

73. Sophie N, Johanne B, Annie J, Thérèse P. Changes in expression of vascular endothelial growth factor and its receptors in neonatal hypoxia-induced pulmonary hypertension. Pediatric Research. 2005;58(2):199-205.
74. Chow J, Ogunshola O, Fan SY, Li Y, Ment LR, Madri JA. Astrocyte-derived VEGF mediates survival and tube stabilization of hypoxic brain microvascular endothelial cells in vitro. Brain Research Developmental Brain Research. 2001;130(1):123-32.
75. Proescholdt MA, StevenJacobson, NancyTresser, Oldfield EH, Merrill MJ. Vascular Endothelial Growth Factor Is Expressed in Multiple Sclerosis Plaques and Can Induce Inflammatory Lesions in Experimental Allergic Encephalomyelitis Rats. JouRNAl of Neuropathology & Experimental Neurology. 2002;61(10):914-25.
76. Gerber HP, Malik AK, Solar GP, Sherman D, Liang XH, Meng G, et al. VEGF regulates haematopoietic stem cell survival by an inteRNAl autocrine loop mechanism. Nature. 2002;417(6892):954-8. Epub 2002/06/28.
77. Santos SC, Dias S. InteRNAl and exteRNAl autocrine VEGF/KDR loops regulate survival of subsets of acute leukemia through distinct signaling pathways. Blood. 2004;103(10):3883-9. Epub 2004/01/17.
78. Ohba T, Cates JM, Cole HA, Slosky DA, Haro H, Ando T, et al. Autocrine VEGF/VEGFR1 signaling in a subpopulation of cells associates with aggressive osteosarcoma. Molecular cancer research : MCR. 2014;12(8):1100-11. Epub 2014/04/25.
79. Lichtenberger BM, Tan PK, Niederleithner H, Ferrara N, Petzelbauer P, Sibilia M. Autocrine VEGF signaling synergizes with EGFR in tumor cells to promote epithelial cancer development. Cell. 2010;140(2):268-79. Epub 2010/02/10.
80. Luisa M. Cyclooxygenase-2 (COX-2) in inflammatory and degenerative brain diseases. J Neuropathol Exp Neurol. 2004;63(9):901-10.
81. Minghetti L. Cyclooxygenase-2 (COX-2) in inflammatory and degenerative brain diseases. J Neuropathol Exp Neurol. 2004;63(9):901-10.
82. Bianchi R, Giambanco I, Donato R. S100B/RAGE-dependent activation of microglia via NF-kappaB and AP-1 Co-regulation of COX-2 expression by S100B, IL-1beta and TNF-alpha. Neurobiology of Aging. 2010;31(4):665-77.
83. Bianchi R, Adami C, Giambanco I, Donato R. S100B binding to RAGE in microglia stimulates COX-2 expression. J Leukoc Biol. 2007;81(1):108-18.
84. Shanmugam N, Kim YS, Lanting L, Natarajan R. Regulation of cyclooxygenase-2 expression in monocytes by ligation of the receptor for advanced glycation end products. JouRNAl of Biological Chemistry. 2003;278(37):34834.
85. Hiscott J, Marois J, Garoufalis J, D'Addario M, Roulston A, Kwan I, et al. Characterization of a functional NF-kappa B site in the human interleukin 1 beta promoter: evidence for a positive autoregulatory loop. Molecular & Cellular Biology. 1993;13(10):6231-40.
86. Li Y, Barger SW, Ling L, Mrak RE, Griffin WST. S100 Induction of the Proinflammatory Cytokine Interleukin-6 in Neurons . JouRNAl of Neurochemistry. 2010;74(1):143-50.

87. Yan SD, Schmidt AM, Anderson GM, Zhang J, Brett J, Zou YS, et al. Enhanced cellular oxidant stress by the interaction of advanced glycation end products with their receptors/binding proteins. JouRNAl of Biological Chemistry. 1994;269(13):9889-97.
88. Howes KA, Liu Y, Dunaief JL, Milam A, Frederick JM, Marks A, et al. Receptor for advanced glycation end products and age-related macular degeneration. Investigative Ophthalmology & Visual Science. 2015;45(10):3713.
89. Kidambi S, Lee I, Chan C. Primary Neuron/Astrocyte Co-Culture on Polyelectrolyte Multilayer Films: A Template for Studying Astrocyte-Mediated Oxidative Stress in Neurons. Advanced Functional Materials. 2010;18(2):294-301.
90. Gomes, F. CA, Spohr, T. CLS, Martinez, Neto M. Cross-talk between neurons and glia: highlights on soluble factors. Brazilian JouRNAl of Medical & Biological Research. 2001;34(5):611.
91. Tomaselli KJ, Neugebauer KM, Bixby JL, Lilien J, Reichard LF. N-cadherin and integrins: Two receptor systems that mediate neuronal process outgrowth on astrocyte surfaces. Neuron. 1988;1(1):33-43.

Figures

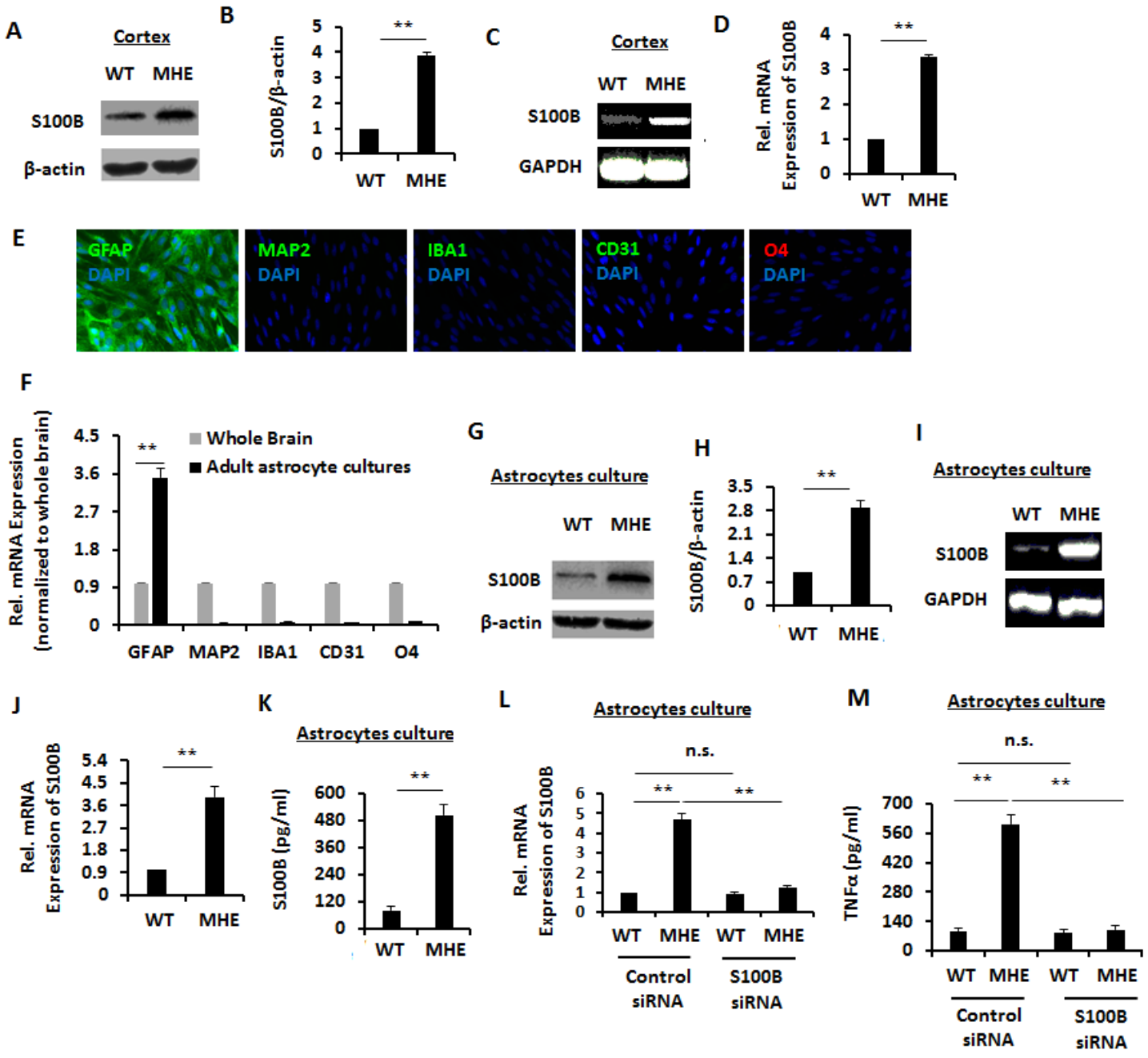

Figure 1

Astrocytes from MHE rats overexpress S100B. (A, B) Immunoblot analysis and densitometry of cortical homogenates from MHE rats with antibodies against S100B and β-actin. (C, D) Analysis for S100B mRNAs of cortical homogenates from MHE rats by qPCR. (E) Cultured astrocytes were plated on coverslips and stained for cell-specific markers (GFAP, MAP2, IBA1, CD31, and O4) for detection of astrocytes, microglia, endothelial cells, and oligodendrocytes, respectively. (F) Cell-specific genes were measured by RT-PCR in astrocyte culture compared to expression levels in whole brain homogenates. (G, H) Immunoblot analysis and densitometry of lysates from MHE astrocytes culture using anti-S100B and β-actin antibodies. (I, J) Analysis for S100B mRNA of MHE astrocytes culture by qPCR. (K) ELISA assay for S100B level of supernatants from MHE astrocytes culture. (L) Analysis for S100B mRNA of MHE

astrocytes culture transfected with S100B siRNA by qPCR. (M) ELISA assay for TNFα level of supernatants from MHE astrocytes culture transfected with S100B siRNA. Data are shown as mean± SD. *P <0.05, **P <0.01. n.s., not significant. scale bar, 25 μm. MRGD, merged image.

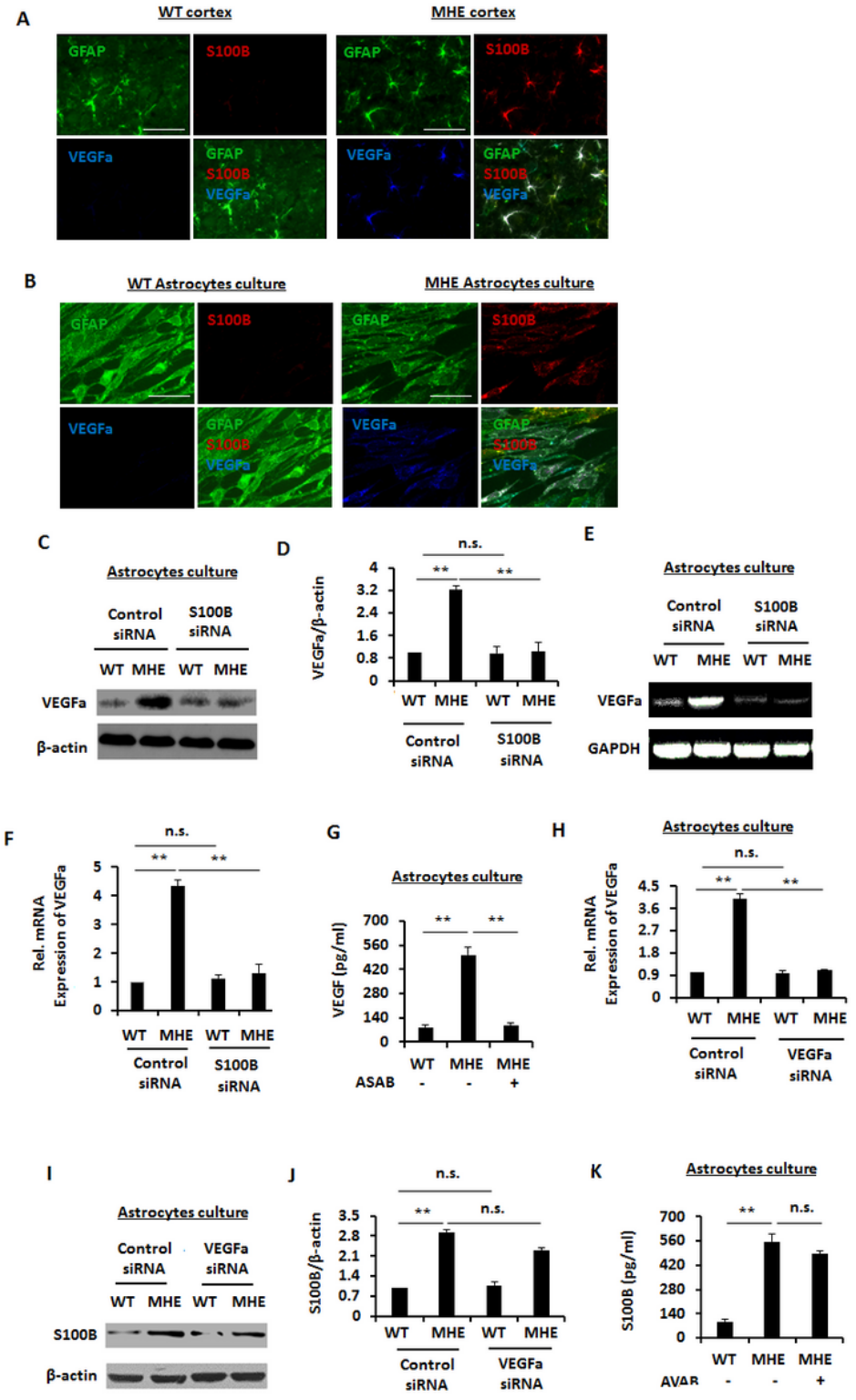

Figure 2

Autocrine S100B induces VEGF production in MHE astrocytes. (A) Immunostaining of free-floating coronal sections from MHE rats using antibodies against VEGF-A (red), S100B (blue), GFAP (green). (B)

Immunostaining of MHE astrocytes culture using antibodies against VEGF-A (red), S100B (blue), GFAP (green), S100B. (C, D) Analysis for VEGF-A mRNA of MHE astrocytes culture transfected with S100B siRNA by qPCR. (E, F) Immunoblot analysis and densitometry of lysates from MHE astrocytes culture transfected with S100B siRNA using anti-VEGF-A and β-actin antibodies. (G) ELISA assay for VEGF level of supernatants from MHE astrocytes culture treated with anti-S100B antibody (ASAB). (H) Analysis for VEGF mRNA of MHE astrocytes culture transfected with VEGF siRNA by qPCR. (I, J) Immunoblot analysis and densitometry of lysates from MHE astrocytes culture transfected with VEGF siRNA using anti-S100B and β-actin antibodies. (K) ELISA assay for S100B level of Supernatants from MHE astrocytes culture treated with anti-VEGF antibody (AVAB). Data are shown as mean± SD. *P <0.05, **P <0.01. n.s., not significant. scale bar, 25 μm. MRGD, merged image.

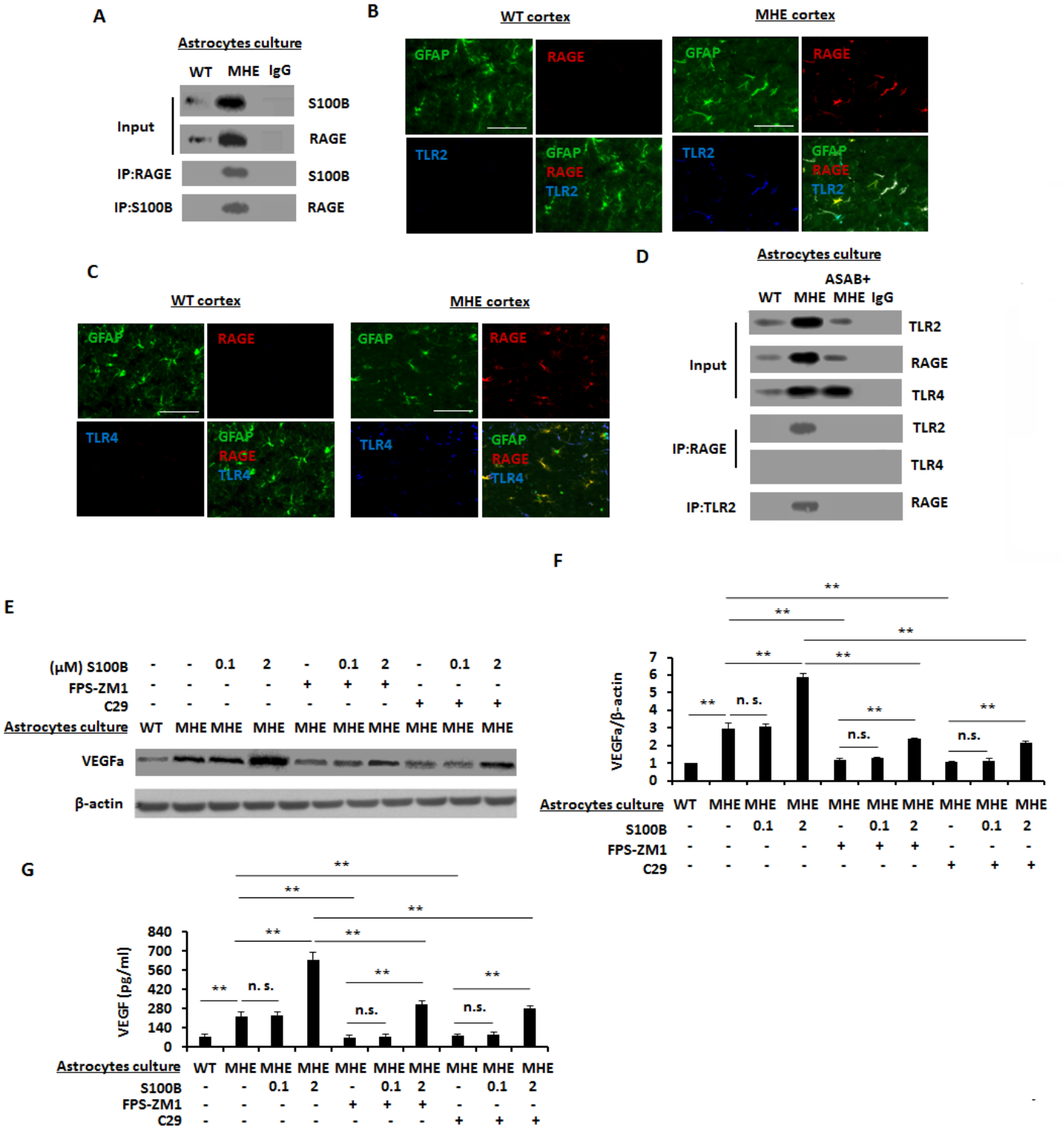

Figure 3

Autocrine S100B by astrocytes facilitates TLR2 and RAGE interaction to elicit VEGF production. (A) Co-immunoprecipitation analysis for the association between RAGE and S100B of lysates of MHE astrocytes culture. (B) Immunostaining of free-floating coronal sections from MHE rats using antibodies against RAGE (red), TLR2 (blue), GFAP (green). (C) Immunostaining of free-floating coronal sections from MHE rats using antibodies against RAGE (red), TLR4 (blue), GFAP (green). (D) Co-immunoprecipitation

analysis for the association between RAGE and TLR2/4 of lysates from MHE astrocytes culture treated with ASAB. (E, F) Immunoblot analysis and densitometry of lysates from MHE astrocytes culture treated with FPS-ZM1 or C29 in the preincubation of S100B (0.1 or 2μM) using anti-VEGF-A and β-actin antibodies. (G) ELISA assay for VEGF level of supernatants from MHE astrocytes culture treated with FPS-ZM1 or C29 in the preincubation of S100B (0.1 or 2μM). Data are shown as mean± SD. *P <0.05, **P <0.01. n.s., not significant. scale bar, 25 μm. MRGD, merged image.

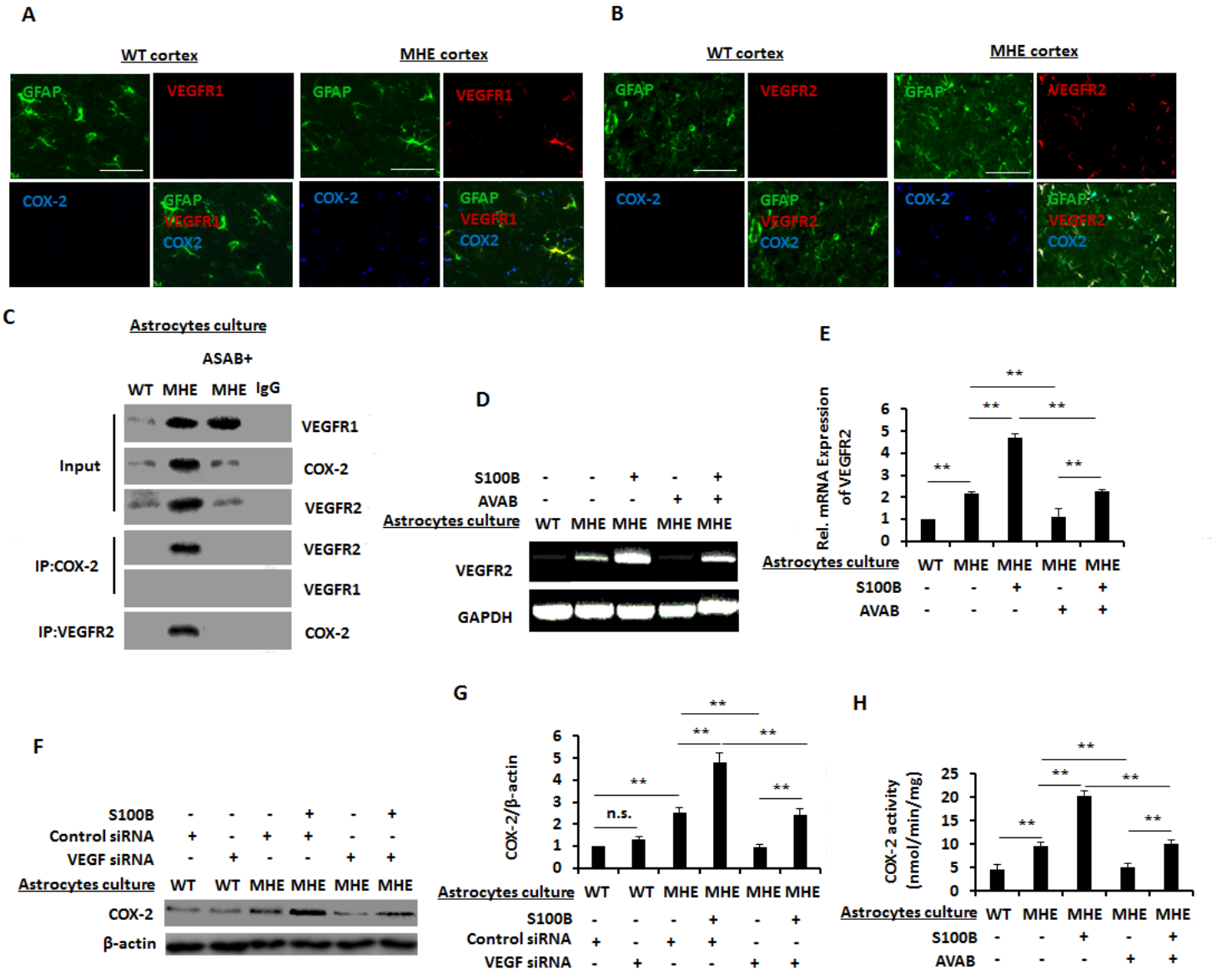

Figure 4

S100B-mediated VEGF autocrine stimulates the interaction of VEGFR2 with COX-2 by astrocytes. (A) Immunostaining of free-floating coronal sections from MHE rats using antibodies against COX-2 (red), VEGFR1 (blue), GFAP (green). (B) Immunostaining of free-floating coronal sections from MHE rats using antibodies against COX-2 (red), VEGFR2 (blue), GFAP (green). (C) Co-immunoprecipitation analysis for the association between COX-2 and VEGFR1/2 of lysates from MHE astrocytes culture treated with ASAB. (D, E) Analysis for VEGFR2 mRNA of lysates from MHE astrocytes culture treated with AVAB in the presence

of 2μM S100B by qPCR. (F, G) Immunoblot analysis and densitometry of lysates from MHE astrocytes culture with VEGF siRNA transfection in the presence of 2μM S100B using anti-COX-2 and β-actin antibodies. (H) Assay of COX-2 activity of lysates from MHE astrocytes culture treated with AVAB in the presence of 2μM S100B. Data are shown as mean± SD. *P <0.05, **P <0.01. n.s., not significant. scale bar, 25 μm. MRGD, merged image.

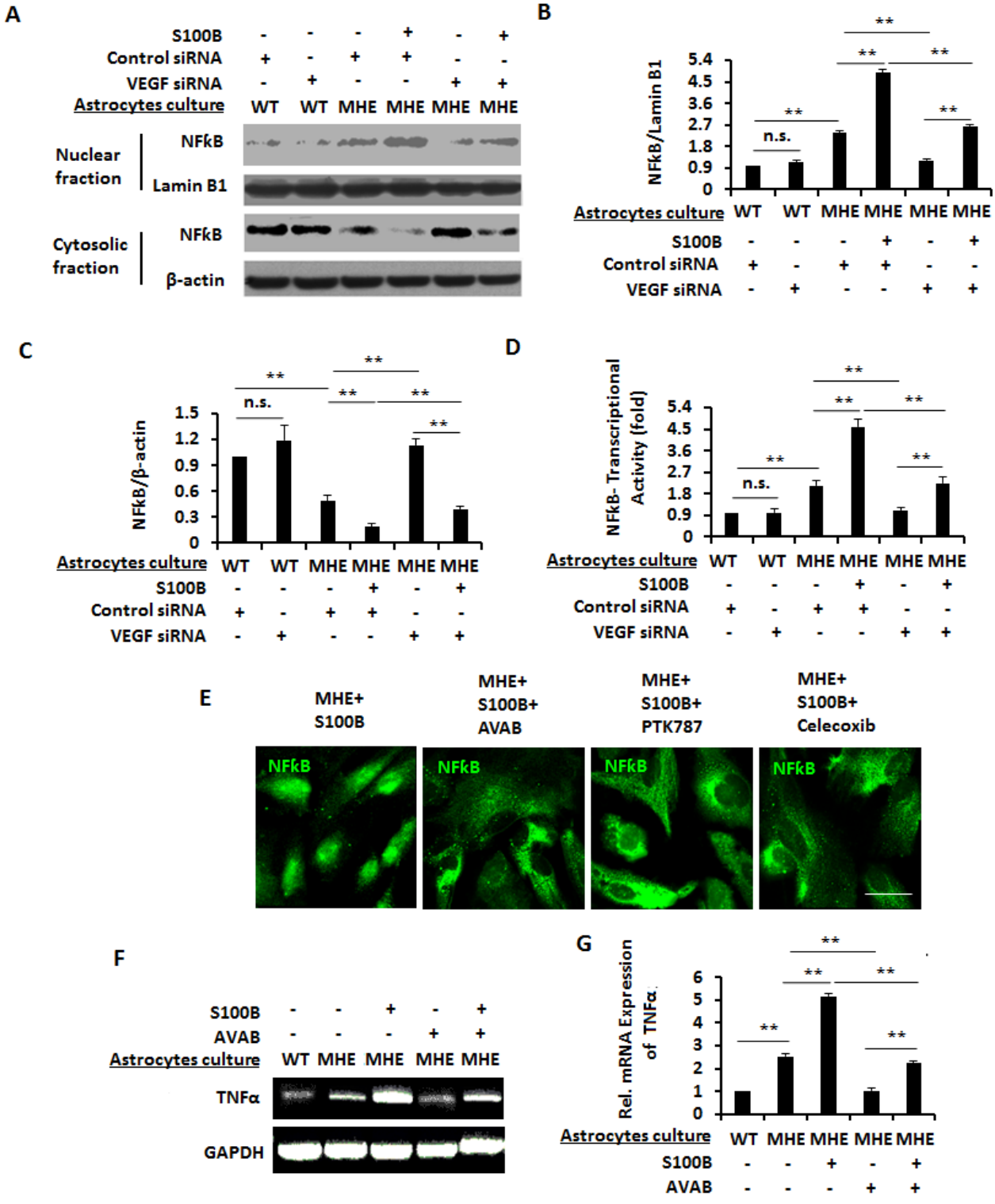

Figure 5

VEGF mediation is required for autocrine S100B-induced inflammation by astrocytes. (A-C) Immunoblot analysis and densitometry of nuclear/cytosolic fraction lysate from MHE astrocytes culture with VEGF siRNA transfection in the presence of 2μM S100B using anti-NF□B and lamin B1/β-actin antibodies. (D) Assay for NF□B transcriptional activation of MHE astrocytes culture with VEGF siRNA transfection in the presence of 2μM S100B via a luciferase reporter construct. (E) Immunostaining of MHE astrocytes culture treated with AVAB, PTK787, or celecoxib in the presence of 2μM S100B using antibodies against NF□B (green). (F, G) Analysis for TNFα mRNA of MHE astrocytes culture treated with AVAB in the presence of 2μM S100B by qPCR. Data are shown as mean± SD. *P <0.05, **P <0.01. n.s., not significant. scale bar, 25 μm. MRGD, merged image.

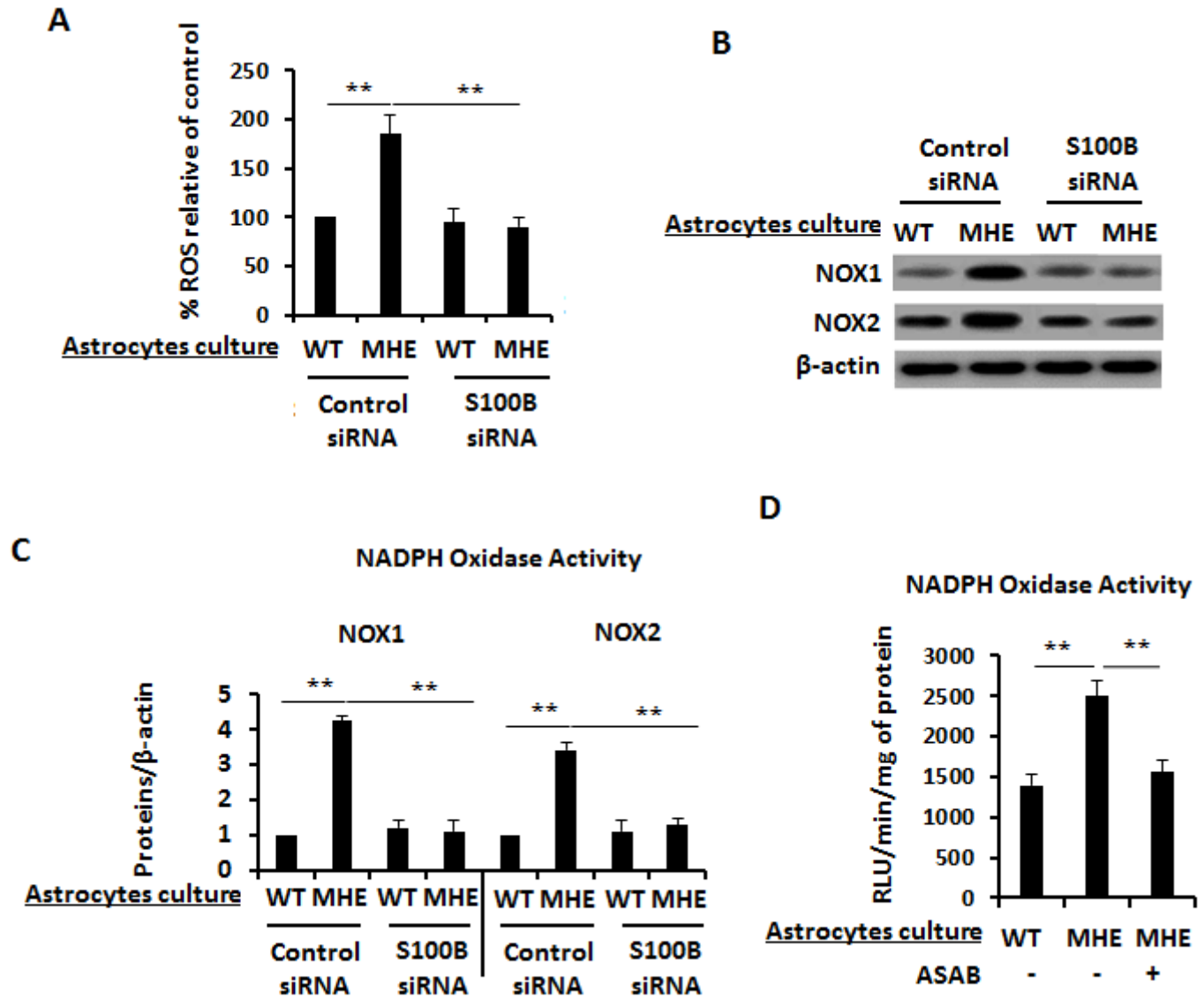

Figure 6

Autocrine S100B stimulates oxidative stress by astrocytes. (A) Assessment of ROS of lysate from MHE astrocytes culture transfected with S100B siRNA. (B, C) Immunoblot analysis and densitometry of lysates from MHE astrocytes culture transfected with S100B siRNA using anti-NOX1/NOX2 and β-actin

antibodies. (D) Assessment of NADPH oxidase activity of lysate from MHE astrocytes culture treated with ASAB. Data are shown as mean± SD. n.s., not significant. *P <0.05, **P <0.01.

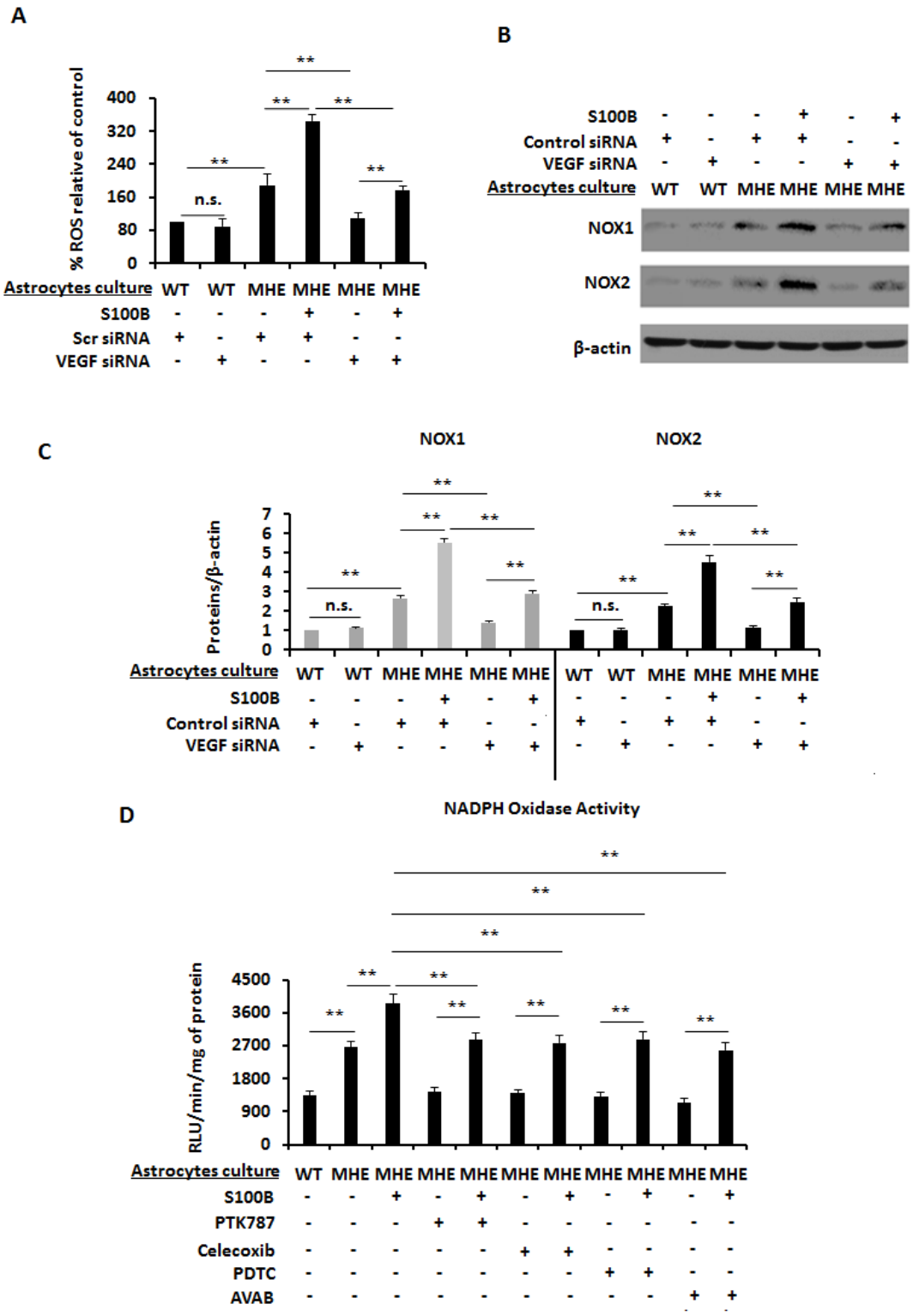

Figure 7

S100B stimulates oxidative stress through VEGF mediation by astrocytes. (A) Assessment of ROS of lysate from MHE astrocytes culture with VEGF siRNA transfection in the presence of 2μM S100B. (B, C) Immunoblot analysis and densitometry of lysate from MHE astrocytes culture with VEGF siRNA

transfection in the presence of 2μM S100B using anti- NOX1/NOX2 and β-actin antibodies. (D) Assessment of NADPH oxidase activity of lysate from MHE astrocytes culture treated with PTK787, celecoxib, PDTC, or AVAB in pre-incubation of 2μM S100B. Data are shown as mean± SD. *P <0.05, **P <0.01.

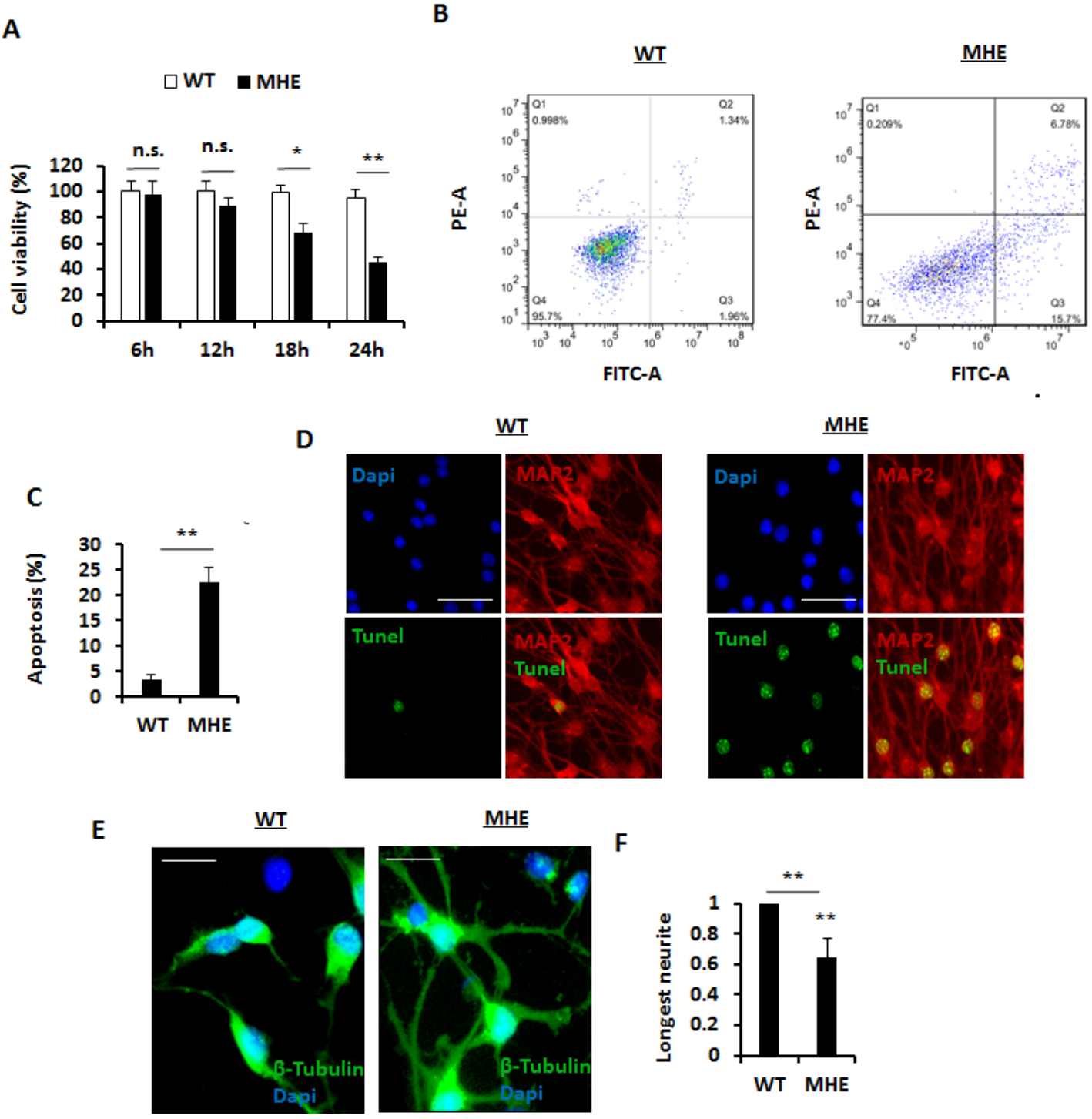

Figure 8

MHE astrocytes show impairment in supporting neuronal growth. (A) Cell viability assay of N2A cells in coculture of MHE astrocytes culture using methylene blue staining. (B) Representative flow cytometric

dot-plots of N2A cells in coculture of MHE astrocytes culture. (C) Flow cytometric quantification of the percentage of apoptotic N2A cells in coculture of MHE astrocytes culture. (D) Immunostaining of primary cultured cortical neurons in coculture of MHE astrocytes culture using antibodies against DAPI (blue), TUNEL (green), MAP2 (red). (E) Immunostaining of primary cultured cortical neurons in coculture of MHE astrocytes culture using antibodies against DAPI (blue), β-tubulin (green). (F) Measurement of longest neurite in each neuron in coculture of MHE astrocytes culture. Data are shown as mean± SD. *P <0.05, **P <0.01. n.s., not significant. scale bar, 25 μm. MRGD, merged image.

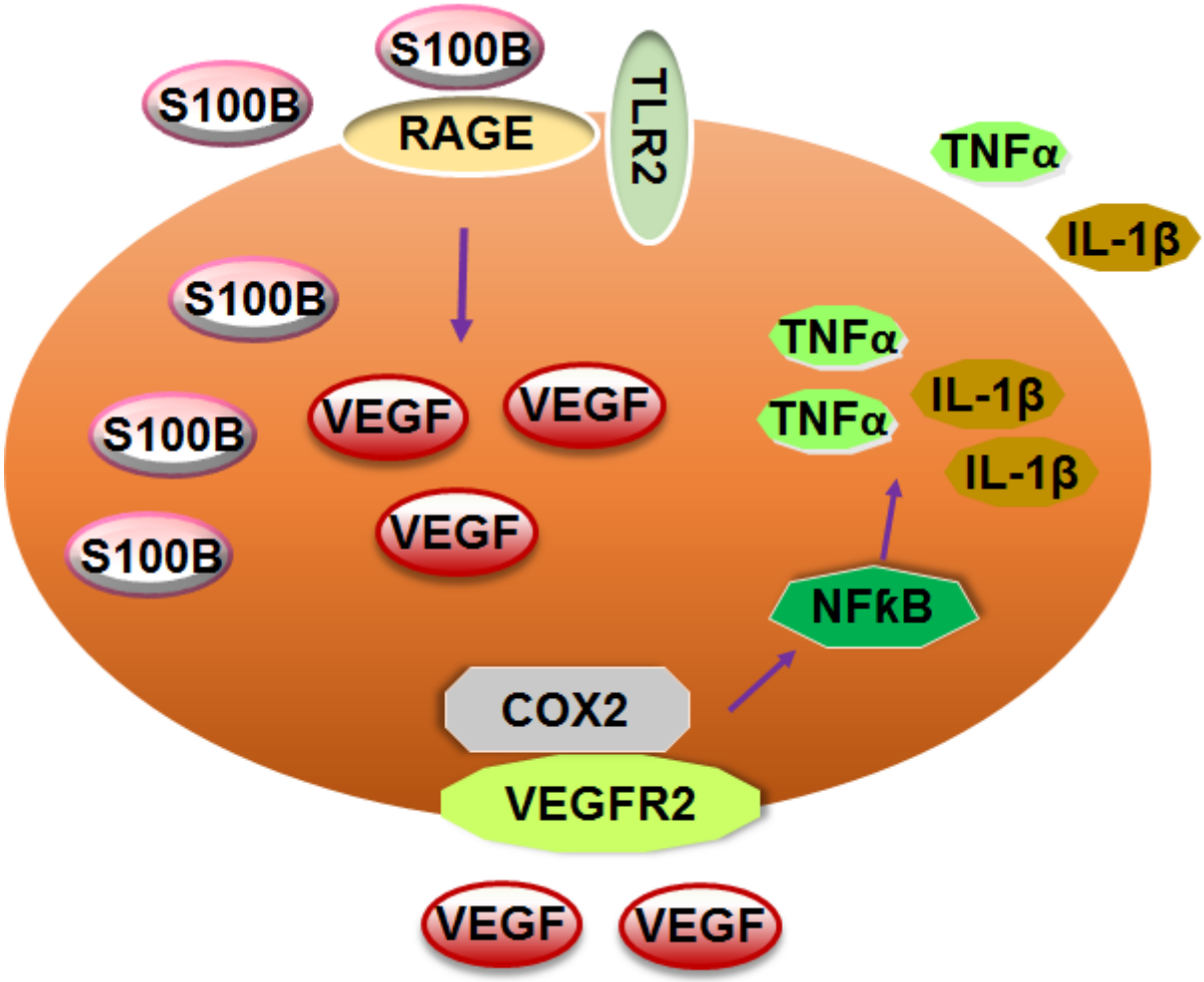

Figure 9

S100B-VEGF autocrine signaling pathway. Astrocytes-derived S100B initiates its autocrine effects by binding to RAGE; activated RAGE interacts with TLR2, which stimulates VEGF expression and secretion. Autocrine VEGF leads to the interaction of VEGFR2 and COX-2, and activation of COX-2. Once activated, COX-2 recruits NF□B to translocate into the nucleus, which triggers inflammatory cytokines production.